



Published in final edited form as:

Angew Chem Int Ed Engl. 2012 July 23; 51(30): 7396–7417. doi:10.1002/anie.201201040.

Smart Self-Assembled Hybrid Hydrogel Biomaterials

Prof. Dr. Jindřich Kopeček and

Department of Pharmaceutics and Pharmaceutical Chemistry, Department of Bioengineering, University of Utah Salt Lake City, Utah 84112 (USA)

Prof. Dr. Jiyuan Yang

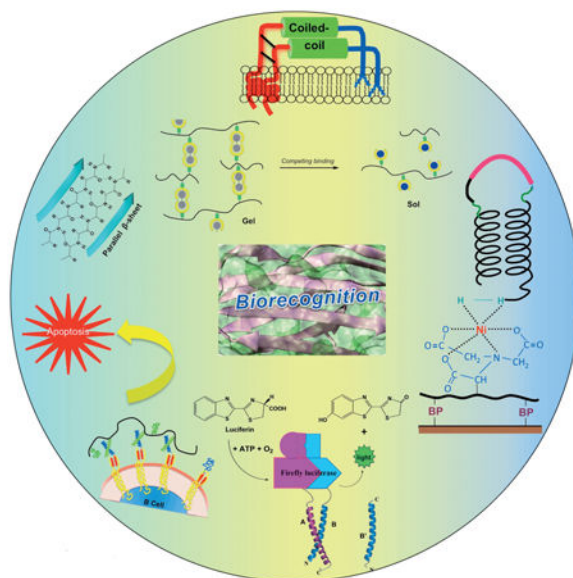
Department of Pharmaceutics and Pharmaceutical Chemistry, Department of Bioengineering, University of Utah Salt Lake City, Utah 84112 (USA)

Jindřich Kopeček: jindrich.kopecek@utah.edu

Abstract

Hybrid biomaterials are systems created from components of at least two distinct classes of molecules, for example, synthetic macromolecules and proteins or peptide domains. The synergistic combination of two types of structures may produce new materials that possess unprecedented levels of structural organization and novel properties. This Review focuses on biorecognition-driven self-assembly of hybrid macromolecules into functional hydrogel biomaterials. First, basic rules that govern the secondary structure of peptides are discussed, and then approaches to the specific design of hybrid systems with tailor-made properties are evaluated, followed by a discussion on the similarity of design principles of biomaterials and macromolecular therapeutics. Finally, the future of the field is briefly

Graphical abstract



Keywords

hybrid biomaterials; hydrogels; molecular recognition; protein structures; self-assembly

1. Introduction

Self-assembly is omnipresent in nature at both macro- and microscales; it describes the spontaneous association and organization of numerous individual units into rational and well-defined structures without external participation.^[1,2] Molecular biorecognition is at the center of all biological processes. It forms the basis for the design of precisely defined smart systems, including targeted therapeutics, imaging agents, stimuli-sensitive and self-assembled biomaterials, and biosensors.

Biorecognition-based self-assembly is an efficient method for building new supramolecular architectures. It permits the design of materials programmed at nanometer to micrometer scales.^[3,4] Combination of self-assembly at different length scales leads to structural hierarchies.^[5–7] For example, a collagen fiber results from the hierarchical organization spanning from the nanoscale to macroscale: three collagen macromolecules form one triple helix; multiple triple helices assemble into fibrils that in turn align to form a mature collagen fiber.^[8]

Hydrogels are the first biomaterials designed for biomedical use.^[9] They are materials with a distinct three-dimensional structure that swell but do not dissolve in water. Their classification may be based on the source (natural and synthetic hydrogels), on the nature of cross-linking (covalent or physical hydrogels), on the nature of the network (homopolymer networks, copolymer networks, interpenetrating networks, and double networks), and on their fate in the organism (degradable and non-degradable hydrogels).^[10,11] Numerous Reviews on various aspects of hydrogel science are available;^[10–25] consequently, this Review focuses on self-assembled biomaterials/hydrogels from genetically engineered polymers and on hybrid hydrogels composed from at least two distinct classes of macromolecules, for example, synthetic and biological macromolecules interconnected either covalently or noncovalently. To restrict the scope further, we shall discuss only peptides and proteins as natural components of hybrid systems.

2. Basic Scientific Principles Governing the Self-Assembly of Peptides

2.1. Coiled-Coils

The coiled-coil is one of the basic folding patterns of native proteins. It consists of two or more right-handed α -helices winding together to form a slightly left-handed super-helix.^[26–29] The primary structure of the coiled-coil motif is characterized by a sequence of repeating heptads designated as [a,b,c,d,e,f,g]_x, in which a and d are usually hydrophobic amino acid residues, while the others are polar. Two helices associate through a hydrophobic interface between a and d, making b, c, and f face outward. Interhelical electrostatic interactions between residues e and g contribute to the stability of the coiled-coil. Depending on their detailed structure, α -helices may associate as homodimers, heterodimers in parallel

or antiparallel alignments, or form higher order (for example tetramer) aggregates (Figure 1).^[30–32]

Hundreds of native proteins, such as muscle proteins, transcription factors, cytoskeletal proteins, cell and viral surface proteins, tumor suppressors, molecular motors, and many disease- and organ-specific auto-antigens have coiled-coil domains.^[33] The coiled-coil domains play important roles in the specific function of these proteins. A distinctive feature of coiled-coils is the specific spatial recognition, association, and dissociation of helices, making it an ideal model for protein biomaterials in which the higher order structures may be predicted based on the primary sequence. Various functional groups may be exactly positioned into the coiled-coil structure, allowing specific intermolecular interactions to occur.

The typical α -helix is right-handed, and 3.6 amino acid residues are needed to form a full turn. In a left-handed coiled-coil (composed of right-handed helices), one heptad forms exactly two turns (a so-called 7/2 repeat—7 amino acids per 2 turns). In nature, coiled-coils with different periodicities, for example, 11-residues periodicities, or with insertions of one or more residues into the heptad pattern can be found (insertions of one residue are called skips, three-residues insertions stammers, and four residue insertions are stutters).^[26,34] The most frequent forms in nature are dimers, trimers, and tetramers; however, the formation of multimers and more complex assemblies is well-known.^[35] A new coiled-coil design, a de novo peptide that forms a six-helix bundle with a central channel that permits passage of water molecules, was recently described.^[36] The versatility of the coiled-coil motif, especially the possibility to manipulate its stability and specificity by modifying the primary structure (up to 10^{-15} M stabilities may be achieved^[37]), bodes well for their use in the successful design of new biomaterials.

From the point of view of the design of new, coiled-coil-containing materials, the known relationship between the structure of coiled-coil-forming sequences and their recognition, association, and folding is a great advantage. Apparently, owing to the repetitiveness of the sequence, the α -helix is the only type of secondary structure in coiled-coils.^[38] Mutations result either in total disruption of the secondary structure or the structure is preserved. On the contrary, there are many variations in the tertiary/quaternary structure of coiled-coils. The number of strands can alter between 2, 3, 4, and 5, and the orientation between the helices can be parallel or antiparallel.^[39] These structural variations correspond with different biological functions.

Interaction of left-handed and right-handed α -helices (30 amino acid residues each) with peptides containing D- and L-amino acids was evaluated.^[40] The helical net diagram predicted that two helices of a D/L structure will pack at a packing angle of 0° , in contrast to natural L/L coiled-coils where the helices cross at 20° . The two peptides, D-Acid and L-Base, formed stable heterotetramers exhibiting features of both specific and nonspecific packing.^[40]

There are several examples of chirality-independent peptide/protein recognition. Glycophorin A (GPA) transmembrane domain peptides have demonstrated lack of

stereospecificity in GPA helix–helix interactions.^[41] Kolluri et al. have shown that a Nur77-based peptide and its enantiomer bind to the Bcl-2 loop, converting Bcl-2 from a protector into a killer of cancer cells. Both stereoisomers of this nonapeptide (FSRSLRSLL) act as molecular switches to displace the Bcl-2 BH4 domain, exposing its BH3 domain that blocks the antiapoptotic activity of Bcl-X_L.^[42]

Such studies provide a scientific basis for the design of D-peptide inhibitors of helical L-protein targets.^[40,43,44] One of the suitable screening methods to identify D-peptides that bind to specific targets is mirror-image phage display.^[45]

2.2. β -Sheets

β -Sheets are important structural elements in proteins. β -Strands are aligned adjacent to each other and are stabilized by hydrogen bonds between the carbonyl oxygen of an amino acid in one strand and the backbone amide of a second amino acid in another strand. The strands (at least two, but frequently more^[46,47]) can arrange in parallel or antiparallel fashion to form the β -sheets. The stability of β -sheets depends on the interaction of side chains of neighboring amino acids.^[1,48] These interactions must compensate for the loss of translational and solvation energies of the peptide (Figure 1).^[49]

Studies of homochiral and heterochiral interactions between enantiomeric β -sheets indicated that homochiral pairing is strongly preferred.^[50] Similarly, triblock-type amphiphilic oligopeptides composed of D- or L-tetraleucine domains flanking pH-responsive L- or D-octalysine segments self-assembled into β -sheet structures with opposite chirality. AFM studies revealed that homochiral solutions self-assembled into amyloid-type nanofibers, whereas the racemic mixture formed only globular aggregates.^[51]

Interactions of D- and L-amino acid β -sheet-forming peptides have demonstrated biological relevance. The polymerization of the amyloid β -peptide (A β) has been identified as the major factor during Alzheimer's disease pathogenesis. A 12-residue D-peptide (QSHYRHISPAQV) was identified that binds to amyloid plaques in brain tissue sections of Alzheimer's patients.^[52] In addition, it decreased the average size of A β aggregates and decreased the A β cytotoxicity toward PC12 cells.^[53]

Zhang et al. have recently evaluated the structural dynamics of a β -sheet-forming 16-residue self-assembling peptide.^[54] At room temperature, the D-EAK16 peptide (AEAEAKAKAEAEAKAK) displayed a typical β -sheet CD spectrum. When the temperature was increased to 80°C, a phase transition to an α -helix occurred without going through a detectable random-coil intermediate. The studies of the effect of temperature, pH, ionic strength, and concentration of denaturation agents revealed that only the thermal behavior of the D-peptide was different when compared to the L-counterpart.^[54] Chiral self-assembling peptide nanofiber scaffolds were formed from both L- and D-peptides.^[55] As expected, peptides composed of alternating D- and L-amino acids self-assembled poorly.^[56] These data seem to indicate that the chirality of peptides does not hinder the formation of well-defined nanostructures.

The β -hairpin is a frequently occurring motif composed of two adjacent antiparallel β -strands joined by a loop. β -Hairpin peptides can form hydrogels after intramolecular folding and intermolecular assembly triggered by external stimuli, such as changes in pH, ionic strength, or temperature.^[57,58] For example, the MAX1 peptide, ((VK)₄-V^DPPPT-(KV)₄-CONH₂), is composed of two strands of alternating K and V residues connected by a tetrapeptide turn sequence. MAX1 folding into a hairpin conformation can be triggered by increase in pH^[58] or in ionic strength.^[59] Complete β -sheet transformation and 3D hydrogel formation at physiological conditions occurs within about 30 min.^[60]

2.3. Stimuli Sensitivity of Coiled-Coils and β -Sheets

The stability of coiled-coils depends on the number of heptads (length of the peptide),^[30] packing at the hydrophobic core (a, d positions),^[61] and interhelical ionic interactions (e, g positions).^[32,62] These interactions depend on environmental factors; consequently, the stability of coiled-coils will be dependent on temperature,^[63] pH,^[64] and ionic strength.^[65] One interesting approach to stimuli sensitivity of coiled-coils is the employment of metal–ligand coordination as the driving force for conformation/association manipulation. Two carboxyl groups in a peptide sequence may form a dirhodium complex and disassemble a coiled-coil dimer in a reversible manner.^[66]

Similarly, the process of β -sheet assembly is driven by intermolecular and intramolecular interactions, including electrostatic, hydrophobic, π -stacking, and hydrogen bonding. As a result, the process is responsive to changes in pH, temperature, and solvents.^[49,67] An important factor is concentration: upon reaching a critical concentration, peptides can self-assemble into tapes, ribbons, fibrils, and fibers.^[68]

2.4. Switch Peptides

Interesting structures have been designed that switch from one secondary structure to another as a response to various stimuli, such as temperature, pH, or concentration. Mutter et al. have shown a pH-dependent switch of an amphiphilic peptide from α -helix to β -sheet.^[69] More recently, they designed a switch peptide that disrupts amyloid-like β -sheet assemblies by converting the peptides into α -helices.^[70] Kokscha et al. synthesized peptide VW19 (LKVELKELKKELVVLKSELKELKKEL) that contains structural elements matching both α -helical folding and β -sheet formation. Depending on the environmental conditions (pH and/or concentration of the peptide), it can assume a random-coil, β -sheet, or coiled-coil conformation.^[71] Similarly, Woolfson et al. designed peptides with structural duality that folded into a parallel leucine-zipper dimer under reducing conditions and a monomeric helical hairpin in an intramolecularly disulfide bridged state.^[72] Secondary structural changes can be combined with assembly into three-dimensional structures: Schneider et al. designed pH-sensitive hydrogels based on a peptide that switches secondary structure from unfolded to amyloid-like assembly.^[58] The impact of metal ions on the transformation between α -helical and β -sheet protein structures was studied using an antiparallel coiled-coil motif containing histidine residues. Addition of Cu²⁺ or Zn²⁺ ions resulted in a decrease of helical content with a concomitant increase of β -sheet content.^[73]

2.5. Impact of Attaching a Linear Synthetic Macromolecule to a Peptide on its Secondary Structure

The impact of attaching a synthetic polymer chain to a coiled-coil-forming peptide on the stability of the construct is an important design factor for hybrid biomaterials. Conjugation of α -methoxypoly(ethylene glycol) (mPEG, molecular weight 2000) to a series of peptides with the general structure (VSSLESK)_n ($n = 3-6$) did not have a disturbing effect on coiled-coil formation, but rather improved the thermal stability of the coiled-coil superstructure.^[74] In a similar study, a coiled-coil forming peptide G-(EAKLAEI)₃Y was modified with PEG (molecular weight 750 and 2000). Although the PEG attachment did not prevent the coiled-coil formation, analytical ultracentrifugation experiments showed a decrease in the relative concentration of coiled-coil aggregates with increasing PEG chain length.^[75]

The impact of attaching a synthetic polymer to a β -sheet forming peptide has also been extensively evaluated.^[67,76,77] Semitelechelic poly(*N*-(2-hydroxypropyl)methacrylamide) (poly(HPMA)) terminated by SH groups was attached to a maleimide-modified β -sheet peptide, QQRFQWQFEQQ. Circular dichroism (CD) spectroscopy and Congo Red binding studies showed that the peptide block imposed its β -sheet arrangement on the structure of the diblock copolymers. Transmission electron microscopy and atomic force microscopy confirmed that both the peptide and the copolymers had the ability to self-assemble into fibrils.^[67] To evaluate the impact of PEG molecular weight on the properties of PEG-peptide conjugates, an amyloid peptide fragment (FFKLVFF) was attached to PEG with molecular weights of 1, 2, and 10 kDa. At elevated concentrations, conjugates with 1 and 2 kDa PEG formed a nematic phase, whereas the conjugate with 10 kDa PEG exhibited a hexagonal columnar phase.^[76] Pluronic F127 micelles were able to stabilize the secondary structure of an entrapped peptide (AKA₃KA)₂, resulting in increase of helicity and decrease of thermal denaturation. Covalent binding of the peptide to Pluronic F127 resulted in self-assembly into hydrogels.^[77] Attachment of PEG (5 or 10 kDa) to alanine-rich polypeptide (ca. 12 kDa) resulted in retardation of β -sheet formation and fibrilization owing to steric interference of PEG and net reduction of attractive interactions between unfolded peptide structures.^[78]

3. Self-Assembled Hybrid Biomaterials

The self-assembly of hydrogels from traditional block and graft copolymers may be driven by hydrophobic interactions, as in ABA block copolymers, where a hydrophilic block B is capped with hydrophobic blocks A.^[79,80] However, designing hydrogel-forming polymers using recognition motifs found in the nature provides methods for the design and synthesis of precisely defined three-dimensional structures.^[81,82] The possibility to initiate self-assembly by an external signal (stimuli sensitivity) is very important to control the final structure.^[83] The high degree of recognition of peptide motifs results in precise spatial arrangement of macromolecules in a 3D structure. Two approaches have been evaluated to design structures that self-assemble into biomaterials and/or hydrogels: peptide/protein-based materials^[84,85] and hybrid systems composed from at least two motifs, namely a synthetic macromolecule and a peptide/protein motif.^[63,86-91] Achievements reached in these areas will be covered below.

3.1. Genetically Engineered Copolymers

The first attempt to synthesize a genetically engineered polymer was reported by Doel et al.^[92] Clones containing genes coding for up to 150 repeats of aspartyl phenylalanine were produced. The polymeric inserts were processed in *E. coli* to create an enzymatically degradable polymer to produce the artificial sweetener Asp-Phe. Cappello et al. then designed numerous materials by combination of motifs from natural biomolecules.^[93,94] The first protein polymer was designed from two oligopeptide blocks: a six amino acid block from silk fibroin (GAGAGS) and a 10 amino acid block from human fibronectin (VTGRGDSPAS). The hexamer block was chosen owing to its propensity to produce stable (β -sheet structure; the decapeptide was selected for its cell attachment properties. Ghandehari, Capello, and co-workers evaluated protein polymers composed of tandemly arranged silk-like blocks (GAGAGS) and elastin-like blocks (GVGVP) and their self-assembly into hydrogels.^[95–103] The silk-like blocks form hydrogen-bonded (β -sheets that crystallize spontaneously, which imparts thermal and chemical stability. The inclusion of elastin-like blocks decreases the crystallinity and increases the flexibility and water solubility of the copolymers. The introduction of an ionizable residue (glutamic acid) into the silk-elastin-like protein polymers increased the pH- and temperature sensitivity.^[99] Apart from environmental conditions (pH, temperature, ionic strength), the surface characteristics influences intermolecular interactions and thus plays an important role in self-assembly.^[104] Evaluation of the swelling and transport properties of the silk-elastin-like hydrogels suggested that they have the potential to become matrices for controlled release of bioactive materials.^[95,98,100–103]

Temperature-sensitive elastin-based hydrogels composed of repeating pentapeptide motifs, (VPGVG)_x-(VPGXG)_y were designed and synthesized.^[105,106] Their inverse temperature transition can be manipulated by changing protein composition, degree of ionization, pH, salt, or phosphorylation.^[105] At low temperatures, the protein chains remain extended, because of the surrounding pentagonal water cages. As the temperature increases (usually above 25°C), the water pentagons lose their structure and become bulk water, allowing the protein chains to fold into compact structures.

Manipulation of mechanical properties and phase transition can also be achieved by combination of several elastin-like structural motifs. Wright et al. combined elastin-mimetic sequences, possessing different mechanical properties, into triblock copolymers. Following phase separation from aqueous solution, the copolymers form an elastic hydrogel.^[107] Redesign of these block copolymers to include larger end-block segments resulted in materials that are able to withstand significantly greater loads.^[108]

Tirrell's group succeeded in synthesizing architecturally well-defined polypeptides of predictable solid-state structure. A monodisperse polymer containing 14 repeats of the undecapeptide sequence (AlaGly)₄ProGluGly was prepared.^[109] This was followed by the synthesis of polymers containing up to 54 repeats of the nonapeptide sequence (AlaGly)₃ProGluGly.^[110] These polymers were designed to produce a synthetic lamellar protein that would fold over and back at regular intervals and expose functional groups positioned at the folds. The first design required modification of the structure: the deletion of

proline residue resulted in a well-defined structure with controlled spacing of functional groups at the surface (repeating sequence (AlaGly)_xGluGly; Figure 2).^[111]

The self-assembly of genetically engineered ABA triblock copolymers composed from a random coil block (B), flanked by two coiled-coil forming blocks (A), has been pioneered by Tirrell's group.^[84] The self-assembly occurs as a balance between the oligomerization of the helical ends and swelling of the central water-soluble random coil segment.

Consequently, temperature and/or pH-responsiveness may be achieved by manipulating the amino acid sequence of the coiled-coil domains.^[85,112] Minor modifications in coiled-coil block structure have a strong impact on the stimuli sensitivity of self-assembled hydrogels. For example, the thermal stability of the coiled-coil-containing proteins can be manipulated in a predictable way by substituting amino acids in the coiled-coil domain (Figure 3).^[85]

Intermolecular association of A blocks produces physical cross-links in the hydrogel network. It was shown, however, that the ABA chains have a strong tendency to form intramolecular loops, producing elastically ineffective chains.^[113,114] The continuous rearrangement of the A block associates results in surface erosion of the network. The loop formation can be easily avoided (and the erosion rate controlled) by designing ABC block copolymers, where A and C are coiled-coil-forming blocks that do not associate with each other.^[115]

Heilshorn et al. designed a two-component hydrogel composed of two recombinant protein polymers, each containing multiple repeats of the CC43 WW domain^[116] or its proline-rich PPxY ligand. The 1:1 interaction of ligands is the basis of spontaneous hydrogel formation by mixing the two polymers; the biorecognition is not disturbed by other biomolecules, permitting cell encapsulation.^[117,118]

Poly(amino acid) diblock and triblock copolymers prepared by controlled ring-opening polymerization of Leuchs' anhydrides were extensively studied by Deming and coworkers.^[119–122] Diblock copolypeptide amphiphiles, which are polymers composed of charged (hydrophilic) and hydrophobic blocks of amino acid residues, showed unusual behavior.^[123] Block copolypeptides with poly(L-lysine) or poly(L-glutamic acid) as the hydrophilic block and poly(L-leucine), poly(L-valine), or poly(D/L-leucine) as the hydrophobic block did not form micelles in aqueous solution, but self-assembled into 3D hydrogel structures at very low polymer concentrations. Furthermore, the hydrogels maintained their mechanical strength also at high temperatures and recovered (rearranged) rapidly after stress.^[119] The comparison of gel-forming properties of diblock with triblock copolymers supported the hypothesis that both systems assemble in a similar manner.^[121] The triblock-based hydrogels, however, possessed greater strength and better salt tolerance than hydrogels self-assembled from diblock copolymers.^[120,121] The shape of the polymer chains is an important factor in the hydrogel self-assembly (gelation) process. It was found that α -helical segments were better gelators than β -strands, which in turn were better than random coils. The formation of hydrogels from diblock copolymers at low concentrations is an interesting phenomenon, and could one day supplement tools used for the design, synthesis, and self-assembly of novel biomaterials and drug-delivery systems.^[119,123] An interesting design of a diblock copolymer was created by combination of a polypeptide, poly(γ -benzyl-L-glutamate), with a coiled-coil-forming peptide {G-(EIAALEK)₃}. Depending on the length

of PBLG block (from 36 to 250 residues), the diblock copolymer self-assembled into polymersomes or disk-like micelles.^[124]

Genetically engineered pro-resilin, photo-cross-linked by Tyr-Tyr bonds, produced a hydrogel with high resilience and very high fatigue lifetime.^[125] Artificial elastomeric proteins that mimic the molecular architecture of titin were produced by combination of GB1 and resilin protein domains followed by photochemical cross-linking. This created a biomaterial that is highly resilient at low strains, but extensible and tough at high strain, mimicking the properties of muscle.^[126] Taking inspiration from the structure of numerous extracellular matrix proteins that possess a tandem modular elastomeric structure composed from individually folded domains, Li and co-workers designed protein-based reversible hydrogels. First, they constructed an ABA triblock protein based hydrogel using eight GB1 domains (G₈) arranged in a tandem as the center block and flanked it on both sides with a coiled-coil-forming peptide block.^[127] To overcome two limitations of the first design, namely a fast erosion rate owing to formation of intramolecular loops and high viscosity of the protein solution, they used two complementary peptides (CCE and CCK) that do not self-associate but form antiparallel coiled-coil heterodimers.^[128] To engineer tandem modular protein-based hydrogels, they genetically produced two bi- and trifunctional tandem modular proteins carrying the CCE and CCK sequences, namely CCK-G₄-CCK and CCE-G₅-CCE-G₅-CCE. Upon mixing, the solution of the two proteins can undergo reversible sol–gel transitions as a function of temperature.^[129]

The incorporation of biorecognition moieties into the structure of genetically engineered polymers has also been carried out. Integrin-binding ligands were inserted into genetically engineered biomaterials, namely, silk-based,^[130] elastin-based,^[131–133] and ABA triblock copolymers, where a random sequence (containing three copies of the RGD sequence) was flanked by coiled-coil-forming domains.^[134] Silk-elastin-like protein polymers were modified to include antimicrobial, textile targeting, or UV-protective peptide blocks, thus demonstrating possible applications in industrial biotechnology, personal health care, and biodefense.^[135] Another example of incorporation of biological function into genetically produced biomaterials is the incorporation into dragline spider silk of three different antimicrobial peptides. The spider silk domains maintained the self-assembly features, and the formation of β -sheet mediated the formation of 3D biomaterials.^[136]

3.2. Hybrid Systems

Hybrid biomaterials are usually referred to as systems that possess components from at least two distinct classes of molecules, for example, synthetic polymers and biological macromolecules, that are interconnected either covalently or non-covalently.^[10–15] Conjugation of peptide domains to synthetic polymers may lead to novel materials with properties superior to those of individual components. Compared to synthetic polymers, proteins and protein modules have well-defined and homogeneous structures, consistent mechanical properties, and cooperative folding–unfolding transitions. The peptide domain may impose a level of control over the structure formation at the nanometer level; the synthetic part may contribute to the biocompatibility of the hybrid material. The synergistic

combination of two types of structures may produce new materials that possess unprecedented levels of structural organization and novel properties.^[13,137]

Peptide and/or protein segments have been used to introduce degradability,^[138–140] a temperature-induced phase transition,^[60,83] and sensitivity to the presence of biologically active molecules^[141–143] into hybrid hydrogel structures. The combination of synthetic segments and of protein/peptide segments into self-assembled hybrid materials provides an opportunity to combine and superimpose the properties of the component molecules. The inspiration for such structures is commonly derived from self-assembling systems in nature.

3.2.1. Hybrids of Synthetic Polymers with α -Helical Peptides—The first design of a self-assembling hybrid hydrogel combined biorecognition of a homodimer-forming α -helical motif with an HPMA copolymer.^[63] The important conclusion of this study was the validation of the hypothesis that the properties of a coiled-coil protein motif can be imposed onto the behavior of the whole hybrid hydrogel. The temperatures of the melting point of the peptide motif (segment of the stalk region of the *Drosophila* motor protein, kinesin) and of the phase transition (collapse) of the hybrid hydrogel structure were very similar. A temperature-induced hydrogel collapse was observed that corresponded to the structural transition of the coiled-coil domains from an elongated helix to an unfolded state. This is a new temperature-response mechanism for hydrogels that can be tuned over a wide temperature range by assembling gels with coiled-coils that have different melting temperatures. In this study, the genetically engineered protein motifs were attached to the hydrophilic HPMA copolymer backbone by metal complexation (Histag on the peptide with Ni^{2+} at the side chains of polymer). The structure of the coiled-coil cross-links was complex; the peptide sequences formed homodimers, thus an elastically non-effective “cross-link” could form by dimerization of motifs on the same macromolecule. Consequently, tetramers and higher associates were needed for hydrogel formation. As a result, the collapse of the three-dimensional structure was not reversible. Clearly, new designs were needed.

Triblock ABA copolymers, where the central block was PEG and the A blocks a peptide from the coiled-coil region of fibrin, self-assembled in viscoelastic hydrogel biomaterials. Like other materials of similar design, the hydrogels dissolved in buffer after about 8 days, which is probably due to formation of intramolecular loops.^[144] Sahin and Kück synthesized multiblock high-molecular-weight polymers composed of alternating PEG and coiled-coil-forming peptide segments by conjugation of 3.4 kDa α,ω -disucinimidyl succinate homobifunctional PEG and arginine-rich and glutamic acid-rich coiled-coil-forming peptides. The products retained their capacity to produce heterooligomeric assemblies; they also formed homooligomeric micellar structures.^[145] Collagen peptide-based hydrogels for 3D cell growth were synthesized by cross-linking maleimide-decorated 8-arm PEG star polymer with cysteine-terminated collagen triple-helix-forming peptides.^[146]

A new design of hybrid hydrogels was based on graft copolymers containing a pair of sequences that formed coiled-coil antiparallel heterodimers.^[128,147] It was hypothesized that the antiparallel orientation of heterodimers will contribute to the homogeneity of the self-

assembled hybrid hydrogels owing to unique interchain dimer formation and decreased steric hindrance of the (synthetic) polymer backbone on the “in-register” (fully overlapping) alignment of heterodimers. In other words, the distribution of cross-links in these self-assembled hydrogels will be more uniform than in hydrogels self-assembled from graft copolymers containing homodimer-forming coiled-coil grafts or hydrogels synthesized by traditional methods. Furthermore, the proposed design of the self-assembled hybrid hydrogels possessed a potential to be developed into a two-component in situ gel-forming drug delivery system.

For a peptide pair forming antiparallel heterodimers, two pentaheptad sequences with opposite charge (CCE and CCK, Figure 4) were designed.^[128] Three major stabilizing interactions were taken into account: the hydrophobic interactions in the core, electrostatic attractions across the interface, and helical propensity effects. Val and Leu were chosen for the a and d positions, respectively, because of their high hydrophobicity, ability to pack into the core, and the propensity to promote formation of dimeric coiled-coils in numerous leucine zipper mutants. Charged residues (E and K) were placed at positions e and g. Potentially attractive or repulsive electrostatic interactions between these residues have been shown to influence complementary strand specificity and orientation preference. E occupied e and g positions in one strand (CCE), while in the other strand, CCK, K was placed at e and g positions. This design minimizes the probability of forming homodimers owing to their destabilization by electrostatic repulsions. Moreover, a single residue at g position of the fourth heptad in each strand was substituted with the oppositely charged residue. Orientation preference was thus improved, because all potentially attractive interactions are expected in the antiparallel alignment.^[64,148,149] Positions b and c were filled with S and A residues, respectively. Uncharged residues were used in these positions to avoid electrostatic interactions with adjacent residues at positions e and g. S was chosen to enhance solubility; A possesses high helical propensity and was expected to promote helix formation. K was chosen for position f in the CCE coil and E in the CCK coil to balance the net charge of each peptide and increase solubility. It was reported that buried polar interactions played a key role in structural specificity of coiled-coils; in particular, a single buried polar interaction at the hydrophobic interface of the helices of a coiled-coil was sufficient to impose an antiparallel alignment.^[150] Therefore, N residues were placed at the a and d' positions of the third heptad of the CCE coil and CCK coil, respectively. Finally, the coiled-coil sequences were flanked at the *N*-terminus with the CYGG tetrapeptide spacer to decrease the steric hindrance of the polymer backbone on the formation of antiparallel heterodimers and provide an attachment point.

Regarding the self-assembly of HPMA copolymers containing CCE and CCK grafts into hydrogels, there was no homodimeric association of graft copolymers CCK-P or CCE-P (P is the HPMA copolymer backbone). Individual graft copolymers possessed predominantly a random-coil conformation. However, equimolar mixtures of CCK-P and CCE-P formed coiled-coils spontaneously and self-assembled into hydrogels even at very low (0.1 wt%) concentrations (Figure 5).^[128] Dynamic light scattering (DLS) evaluation^[147] of the time course of self-assembly revealed the effects of concentration and time on the self-assembly process of HPMA graft copolymers. The immediate shift of decay time distribution of the

equimolar mixture of CCE-P and CCK-P to longer decay time indicated instantaneous association of complementary peptides. The normalized intensity autocorrelation functions broadened with time and shifted to longer delay times, indicating slowing of the solution dynamics on approaching the gel point.^[147] CCE and CCK also mediated the self-assembly of genetically produced tandem proteins^[129] (see 3.1).

3.2.2. Hybrids of Synthetic Polymers with β -Sheet Peptides—The self-assembly of hybrid block and graft copolymers composed of synthetic polymer backbones and β -sheet motifs was also investigated.^[67,87,151,152] The I28 immunoglobulin (Ig)-like domain of human cardiac titin was used to cross-link acrylamide copolymers into temperature-sensitive hydrogels. The Ig-like domain is a sandwich of two antiparallel β -sheets; it unfolded with a midpoint of 58°C. Acrylamide-based hydrogels cross-linked with the Ig domain demonstrated positive temperature responsiveness (increase in swelling) above the melting temperature of the cross-links (Figure 6).^[87] A theoretical model describing swelling changes in hydrogels caused by unfolding of cross-links has been described.^[153]

Numerous designs of hybrid block copolymers focused on shorter β -sheet-forming peptides.^[67,154–159] The first example of block copolymers of PEG and a β -sheet-forming peptide was published by Lynn and co-workers.^[156–158] The attachment of PEG (molecular weight 3000) to the C-terminus of residues 10–35 of A β (A β (10–35)) of the amyloid peptide rendered the formation of fibrils, in contrast to native peptide, completely reversible. The hybrid material took on a structure composed of up to six (extended) laminated parallel β -sheets surrounded by the PEG block. Apparently, PEG prevented lateral association of the fibrils, and, therefore, inhibited the irreversible step of fibrillogenesis.^[156–158]

Börner et al. demonstrated the peptide-guided assembly of PEG–peptide conjugates into tape structures.^[159] Klok et al. synthesized block copolymers of amphiphilic β -strand peptide sequences flanked by one or two PEG chains. The PEG conjugation stabilized the β -strand secondary structure as compared to unmodified peptide and reduced the sensitivity of the peptide secondary structure to pH variations.^[154,155] Pechar et al. coupled 9-fluorenylmethoxycarbonyl (Fmoc)-protected PEG (MW \approx 500) to (VPGVG)₄ and (VPAVG)₄, and determined their properties. Whereas the diblock copolymers, PEG-(VPGVG)₄ and PEG-(VPAVG)₄, did not undergo any macroscopic temperature-induced phase transition, the presence of the hydrophobic Fmoc group at the end of peptide or PEG chain-induced reversible thermoresponsive self-association of the molecules.^[160]

A block copolymer of poly(HPMA) (2 and 5 kDa) and a (β -sheet peptide (QRRFQWQFEQQ-NH₂) was prepared by thiol–maleimide coupling reaction. Semitelechelic poly-(HPMA)-SH was synthesized by RAFT polymerization of HPMA followed by post-modification aminolysis. The diblock copolymer was obtained by polymer-analogous reaction with *N*-terminal maleimide-modified (β -sheet peptide. Transmission electron microscopy and atomic force microscopy confirmed that the peptide and block copolymers had the ability to self-assemble into fibrils. Interestingly, the pH of (β -sheet formation was different for free peptide than the polymer conjugate.^[67]

HPMA hybrid graft copolymers were prepared by attachment of *N*-terminal CGG-modified (β -sheet peptide (CGGTTRFTWTFTTT) to poly(HPMA) precursor, which contained pendant maleimide groups. CD spectra showed that the strong tendency of the peptide to self-assemble into β -sheets was retained in the copolymers. Furthermore, β -sheet sensitivity to temperature and pH variations decreased owing to poly(HPMA) shielding effect. Atomic force microscopy and small-angle X-ray scattering showed that copolymer had the ability to self-assemble into fibrils.^[151] Transmission electron microscopy showed that poly(HPMA)-*g*-CGGTTRFTWTFTTT fibrils formed matrices with minimal lateral aggregation, which is dramatically different from the highly laterally aggregated peptide fibrils.^[151] This observation coincided with the FTIR results, which suggested that poly-(HPMA) hindered the twisting of the fibrils formed in copolymer through the antiparallel arrangement of the β -strand peptides. Finally, the ability of a hybrid hydrogel self-assembled from HPMA copolymers and complementary β -sheet grafts (TTRFTWTFTTT-NH₂ and TTEFTWTFETT-NH₂) to act as scaffolds for bone tissue engineering was explored.^[152] The hydrogel displayed anisotropic porosity; thus, besides support for preosteoblast cells, it provided surfaces characterized by epitaxy that favored template-driven mineralization of hydroxyapatite (Figure 7). Long-term viability and proliferation of the cells indicated that this β -sheet-based hybrid hydrogel is not cytotoxic, therefore it could be used as bone scaffold. Such novel nanostructures and hydrogels potentially could be applied successfully in a broad range of biomedical applications, from depots for drug delivery, to scaffolds for cell delivery and tissue engineering.

3.2.3. Hybrids of Synthetic Polymers with Protein Mutants—Hydrogels containing proteins that undergo a substantial conformational change in response to a given stimulus have potential applications in sensing, microfluidics, and miniaturized drug-delivery systems. Daunert and co-workers^[161] synthesized hydrogels with covalently attached *calmodulin*, a calcium binding protein, by copolymerization of acrylamide, *N,N'*-methylenebisacrylamide, calmodulin macromonomer (containing an allyl group), and a polymerizable derivative of phenothiazine. Calmodulin undergoes two conformational changes from the native state: into a dumbbell-like conformation when bound to Ca²⁺, and into a more constrictive conformation when bound to phenothiazine. The hydrogel was responsive to both Ca²⁺ and phenothiazine; its incorporation into a simple microfluidic system demonstrated the potential of the hydrogel to control flow (Figure 8).^[161] Mrksich and co-workers genetically engineered calmodulin to contain two cysteine residues.^[162] This mutant was used as a cross-linker (along with dithiothreitol) of 4-arm PEG that contained acrylate groups. The resulting hydrogels underwent changes in the equilibrium degree of swelling upon binding of calmodulin ligand, trifluoperazine.^[162] Murphy et al. modified calmodulin mutant (T34C, T110C) with poly(ethylene glycol) diacrylate to produce a protein with two polymerizable groups.^[163] The latter was photo-cross-linked into a stimuli-sensitive hydrogel, changing swelling upon exposure to trifluoperazine. Glucose-sensitive hydrogels were synthesized by incorporating glucose/galactose binding protein (GBP) mutant into an acrylamide-based hydrogel. GBP consists of two domains connected by a hinge; upon glucose binding, the two domains rotated toward each other to form a closed state. The GBP containing hydrogel showed a dynamic response in the presence of glucose.^[164]

Hydrogels capable of translating enzyme-substrate recognition induced conformational changes into macroscopic motion were prepared.^[165] The design employs the substrate–enzyme interactions of adenylate kinase with ATP to induce a conformational change with concomitant decrease of the hydrogel volume. *Escherichia coli* adenylate kinase (AKe; EC 2.7.4.3) is a 214-residue, three-domain bacterial enzyme (transferase), which catalyzes the phosphoryl transfer reaction $\text{Mg}^{2+}\cdot\text{ATP}+\text{AMP}\leftrightarrow\text{Mg}^{2+}\cdot\text{ADP}+\text{ADP}$. Upon binding of a substrate (or inhibitor), AKe undergoes a large conformational change. The bulky lid domain closes over the active site to shield it from water, avoid substrate hydrolysis, and facilitate the transfer of the phosphate group (Figure 9). AKe was incorporated into defined hydrogel structures through a thiol–maleimide reaction. Synthetic HPMA copolymers with pendant maleimide groups were chosen as the backbone. The wild-type enzyme has one cysteine at position 77, which can be mutated without loss in activity. To create two attachment points, a triple mutant of adenylate kinase, AKtm (C77S, A55C, V169C) was designed, engineered, and purified. The distance between the C^α atoms of residues 55 and 169 decreases from 29.5 Å in the apo-enzyme to 12.4 Å when forming the enzyme–substrate complex. Furthermore, the SH groups at positions 55 and 169 are easily accessible.^[166] The enzymatic activity of AKtm was examined and shown to be similar to AKe.^[165] Hybrid HPMA-based hydrogels were synthesized in a mold by cross-linking the HPMA copolymer with AKtm alone, or AKtm and additional cross-linking agent dithiothreitol (DTT). A control gel was prepared by cross-linking with DTT only. As hypothesized, when the hydrogels were exposed to ATP (substrate), a conformational transition from an “open” to “closed” conformation occurred, resulting in hydrogel volume change. The collapse of about 5–17% in the hydrogel volume was proportional to the AKtm content. Control gel, cross-linked with DTT only, did not collapse. The degree of hydrogel de-swelling increased with the concentration of the substrate. Repeated exposure of hydrogel to ATP buffer followed by a washing step in ATP-free buffer demonstrated the reproducibility of hydrogel swelling alterations and of the AKtm conformational changes (Figure 9).^[165] The novelty of this design is the combination of biorecognition with a catalyzed chemical reaction, namely the transfer of a phosphate from ATP to AMP. There are numerous enzymes that undergo conformational changes following the binding of a substrate to the active site of an enzyme. Thus, this is a new strategy for hybrid hydrogel design, where a variety of chemical reactions can be combined with biorecognition to transform nanoscale conformational changes into macroscopic motion.

4. Methods for the Structural Analysis of Self-Assembled Hydrogels

In addition to traditional approaches for hydrogel characterization, such as rheology, swelling, determination of stimuli-sensitivity, CD spectroscopy, and analytical ultracentrifugation (AUC), stringent analytical techniques are needed to validate the hypothesis that biorecognition-driven self-assembly of soluble polymers into hydrogels results in precise 3D structures with superior properties when compared to traditional hydrogels. Enhanced effort is needed to develop suitable techniques and to create an experimental data bank, which could be used as a reference.

The questions to answer are challenging. They originate from one of the challenges in self-assembly, that is, to control the self-assembly process and prevent defects in the assembled

structures.^[83] For example, for a hydrogel self-assembled by coiled-coil formation, the questions include: what is the fraction of coiled-coils that assembled in an “in-register” manner (total overlap of heptads); what fraction of coiled-coils acts as elastically effective cross-links; what is the extent of cyclization; and are there any pendent peptide grafts not associated in coiled-coils. Some of the techniques used and conclusions reached are described below.

Using ^{13}C and ^{15}N solid-state NMR spectroscopy, Hong, Tirrell, et al. evaluated the dynamic structure of a hydrogel self-assembled from an ABA triblock copolymer, where the A blocks were coiled-coil-forming domains (six heptads) and B is a random block (rich in A, G, and E). The results indicated differential dynamics between the B block and the A blocks. On a microsecond timescale, the B block was isotropically mobile, while the leucine-zipper A blocks were rigid.^[167] This fits the hydrogel structure, where the B domains act as a swelling agent of the network and the A domain participate in physical cross-links. Hong and Conticello evaluated the conformation of an elastin-mimetic recombinant protein, [(VPGVG)₄(VPGKG)]₃₉, by magic angle spinning (MAS) NMR spectroscopy. The average chemical shifts of the solid protein were similar to the values in solution, suggesting similar conformations.^[168] Kříž and co-workers evaluated the structure of elastin-like polypeptides [poly(GVGVP) and poly(AVGVP); $M_n \approx 10^5$] in aqueous environment using ^1H , ^2H , ^{13}C , and ^{15}N NMR spectra. They were able to detect four different physical states when increasing the temperature: state I (statistically shaped fully hydrated polymer), state II (relatively coiled and globular), state III (tightly coiled, more compact), and state IV (aggregated polymer).^[169] The heterodimeric coiled-coil solution structure of a stable coiled-coil motif IAAL (E3/K3) has been solved using ^1H -NOE NMR and structural restraints.^[170] Kokscha et al. used a combination of fluorescence energy resonance transfer and NMR spectroscopy to solve the structure of coiled-coil heterodimers.^[171] Sahin and Kiick used a combination of NMR, size-exclusion chromatography (SEC), and electrophoretic analysis to decode the structure of block copolymers from PEG and coiled-coil peptides.^[145] These results are encouraging, but a more detailed analysis of self-assembled hydrogels is needed. For example, in hydrogels self-assembled from graft copolymers containing peptide grafts forming antiparallel heterodimers, the following questions need to be answered (as described above) relating to the detailed structure of the 3D network: the fraction of grafts forming cross-links, the fraction of cross-links heterodimers, “in-register” alignment, and the extent of cyclization.^[172]

Dynamic light scattering (DLS) is a very suitable method to investigate the time course of self-assembly. By this technique, continuous molecular weight (hydrodynamic volume) increases in the pre-gelation region may be monitored, and the identification of the sol–gel transition is feasible.^[173] The profile of the homodyne autocorrelation function changes with increasing concentration of associating macromolecules from a stretched exponential function to a power law at the gel point, and the pre-gelation solution dynamics slows down as the gel point is approached.^[173] Both effects are related to the polydispersity of clusters formed by random associations. Coupling effects similar to those that appear in glassy systems may become important at concentrations where smaller clusters partially penetrate

the larger ones. For example, DLS has been used to study the random association of hydrophobically modified water-soluble polymers,^[174] block copolymers composed of elastin-like and poly(ethylene glycol) (PEG) blocks,^[156] and multiblock copolymers.^[175]

Diffusing-wave spectroscopy (DWS) uses dynamic light scattering in the determination of the viscoelastic behavior of a complex fluid. The time evolution of the mean-square displacement of a suspension of particles, acting as hard spheres in a viscoelastic medium, can be related to the frequency-dependent storage and loss moduli of the medium.^[176]

Microrheology is a method for measuring the mechanical properties of a material by monitoring the motion of micrometer-sized tracer particles. Compared to conventional mechanical rheometers, which typically require a milliliter of sample, microrheology requires a small sample volume, which is usually less than 10 μL . In passive microrheology, there is no external driving force applied to the tracer particles; the intrinsic Brownian motion of the particles is used, driven by the thermal energy $k_{\text{B}}T$. The theoretical basis for passive microrheology is a generalized Stokes–Einstein relation (GSER) for materials with viscoelastic properties,^[177–179] which can be presented in the following form:

$$\langle \Delta \tilde{r}^2(s) \rangle = \frac{dk_{\text{B}}T}{3\pi a s \tilde{G}(s)} \quad (1)$$

where $\langle \tilde{r}^2(s) \rangle$ is the Laplace transform of the mean-square displacement (MSD) of the tracer particles $\langle (r(t+\tau) - r(t))^2 \rangle$, d is the dimensionality of the displacement vector (usually 2 in videomicroscopy), s is the Laplace frequency, a is the radius of the particles, and $\tilde{G}(s)$ is the Laplace representation of the complex modulus, which encompasses the storage G' and loss G'' moduli.

Microrheology has been used for the study of the liquid–solid transition during gelation^[138] of block copolymers^[85,112] and hybrid graft copolymers.^[128,151,180,181]

Small-angle neutron scattering is suitable for the determination of volume phase transition and microphase separation, detection of inhomogeneities in hydrogel structure, and structural characterization of super-tough gels.^[182]

Fluorescence resonance energy transfer (FRET) can be used to evaluate the alignment of coiled-coils.^[183,184] For example, the donor (Tyr) can be placed in one helix and the acceptor (Trp) placed in the complementary coiled-coil. Only in-register alignment will result in a strong FRET signal.^[185]

5. Specific Designs

The discussion above provides guidelines on the design of self-assembled hybrid biomaterials. However, for particular applications, different aspects need to be taken into account so that multifunctional materials possess the optimal combination of structural, mechanical, and biological properties.^[186]

5.1. Mimics of the Extracellular Matrix

Biorecognition-based self-assembly of materials has a role to play in the development of functional extracellular matrices (ECMs) owing to the capability to produce 3D arrangements with high fidelity. Hybrid hydrogels have a great potential to serve as matrices for the investigation of cell physiology and for the design of tissue-replacement materials.^[17] They can be prepared in cell compatible conditions and their physicochemical properties can be easily controlled; moreover, cell adhesion ligands can be easily incorporated.^[187–189] The possibility to regulate the porosity and interconnectivity of the 3D hydrogel structure permits concomitant control of gas and nutrient supply in a 3D environment.^[187,190] The control of the mechanical properties of the support has an impact on the differentiation of cells.^[191] To evade physical constraints that obstruct cell proliferation and migration, either materials with sufficient porosity or hydrogels that contain oligopeptide cross-links cleavable by proteases naturally secreted by cells^[192,193] need to be employed.

Bissell's group first clearly demonstrated the difference in 2D and 3D cell culture systems. Human breast epithelial cells developed as tumor cells in 2D culture, but slipped back to normal behavior when cultured in 3D analogues of their native microenvironment.^[194] To demonstrate the impact of nanoscale ligand organization on the regulation of cell function, Mooney and co-workers evaluated alginate hydrogels with varying spacing of the RGD ligand and demonstrated that the bulk island density (number of ligands clustered together at one location) controlled the osteoblast phenotype. Controlling the ligand spacing strongly regulated the adhesion, proliferation, and differentiation of osteoblasts.^[195] Anseth's group modulated the elasticity of polymer substrates in situ and evaluated the effect of elastic modulus on valvular interstitial cell (VIC) activation into myofibroblasts. They demonstrated that myofibroblasts can be deactivated solely by changing the modulus of elasticity of the underlying substrate.^[196] Genetically engineered silk-elastin-like protein (SELP) hydrogels have been shown to support chondrocytic differentiation and cartilage matrix accumulation of human mesenchymal stem cells (hMSCs). The possibility of varying the SELP structure indicates that materials with precisely defined 3D structure can be designed as scaffolds for encapsulation and chondrogenesis of hMSCs.^[197]

5.2. Peptide-Mediated Drug Delivery

Genetically engineered silk-elastinlike protein polymers (SELPs) that self-assemble into hydrogels (see Section 3.1) have been used as matrices for drug delivery. Plasmid DNA delivered from a SELP hydrogel showed 1–3 orders of magnitude higher transfection in a murine model of human breast cancer when compared to naked DNA.^[152] SELP-based hydrogels were also successfully applied in the intratumoral delivery of adenoviruses to solid tumors of the head and neck.^[103,198–202] The results clearly indicated that the recombinant polymers improved the safety of the adenovirus-based therapy.^[201]

Self-assembled hybrid hydrogels may serve as depots for sustained release of therapeutic proteins. With proper kinetics of self-assembly,^[147] the depot can be formed in situ, for example following subcutaneous injection. The challenge is to control the release of the biologically active compound (protein). Schneider and co-workers studied the controlled

release of proteins of different molecular weight and charge from self-assembled hairpin-based MAX8 hydrogel. Release of positively charged and neutral proteins was mainly regulated by the sterics of the network. However, negatively charged proteins interacted strongly with the positively charged hydrogel, thus restricting release.^[203]

Examples of triggers for release include ligand-induced conformational change, ligand-induced decrease of cross-linking density, and erosion in the presence of the corresponding receptor. A ligand-induced protein conformational change within a hydrogel microsphere was utilized to control volume (swelling) change and the release of encapsulated drug. An engineered version of calmodulin (CaM) containing two SH groups was reacted with PEG₅₇₅-diacrylate by a Michael-type addition reaction.^[204] Microspheres were prepared by emulsion polymerization and loaded with VEGF. Ligand (trifluoperazine)-induced CaM conformation changes permitted VEGF release to be manipulated.^[205] An antibiotic sensing hydrogel for the trigger-inducible manipulation of cross-linking density with concomitant release of vascular endothelial growth factor (VEGF) was prepared by attachment of genetically engineered bacterial gyrase subunit B (GyrB) to polyacrylamide followed by cross-linking with the anticoumarin antibiotic, coumermycin. Exposure to novobiocin dissociated the GyrB subunits resulting in a decrease of cross-linking density with concomitant dose- and time-dependent release of entrapped VEGF (Figure 10).^[206] Kiick and co-workers demonstrated receptor-mediated protein release. VEGF (vascular endothelial growth factor) molecules served as elastic cross-links in noncovalently assembled hydrogel networks; these networks, produced by the interaction of star PEG capped with low-molecular-weight heparin and a dimeric heparin-binding VEGF, eroded in the presence of the relevant receptor, releasing VEGF.^[207]

Coiled-coil formation between a peptide graft attached to a synthetic copolymer and a complementary graft containing a biologically active compound has been used for the design of novel drug-delivery systems. Pechar and co-workers used coiled-coil peptides for the attachment of recombinant proteins to HPMA copolymer-based macromolecular therapeutics.^[208] Apostolovic et al. evaluated the uptake and subcellular trafficking in B16F10 cells of HPMA copolymers containing K3 grafts dimerized with E3 peptides terminated in methotrexate.^[209,210] In preparatory work for potential applications in drug delivery, Deacon et al. PEGylated a synthetic peptide FosW and demonstrated that it can form a coiled-coil heterodimer with the c-Jun sequence of the AP-1 transcription factor. As expected, PEG did not sterically hinder hybridization.^[211]

5.3. Biomineralization Matrices

In the attempt to create biomaterials that are able to simulate the structure and properties of the bone and to be actively integrated and remodeled by the body, tissue engineering strategies for bone and cartilage regeneration are continuously improving. Biomimetic scaffolds that imitate the characteristics of the natural extracellular matrix are needed. Hydrogels appear to be suitable as matrices for musculoskeletal engineering owing to their biocompatibility, high water content, viscoelasticity, and their permeability.^[212] In addition to traditional hydrogels,^[213] peptides,^[214] and peptide amphiphiles,^[215] self-assembled

genetically engineered polymers,^[216] and hybrid polymers have potential for success in cartilage regeneration and similar applications.

A new generation of bone scaffolds based on a hybrid hydrogel self-assembled from HPMA graft copolymers containing complementary β -sheet peptides has been designed. It was hypothesized that the gel will be biomineralized, through the formation of bone-like hydroxyapatite, within the β -sheet fibrillar template. This approach would provide the foundation for development of a three-dimensional composite material able to effectively function as a matrix for osteoblast growth and differentiation *in vitro* and *in vivo*.^[152] The advantages of the proposed system, namely fiber-like structure, tunable/programmable design based on the association of the β -sheet domains, and ability of the β -sheets to facilitate the deposition of the hydroxyapatite (Figure 7),^[217,218] will ensure the successful construction of a new platform for bone tissue engineering.

Gungormus et al. used a construct from a β -hairpin forming peptide and a heptapeptide (MLPHHGA) to form hydrogels that would display the peptide from the fibril surface and direct biomineralization.^[219] The peptide was identified by phage display and has been shown to control mineral formation in solution.^[220]

5.4. Sensors and Actuators

Ghosh and co-workers designed a family of turn-on protease biosensors based on an autoinhibited coiled-coil switch. The biosensor is composed of three modular domains: a split reporter protein, an antiparallel heterodimeric coiled-coil, and a protease-sensitive linker. Initially, the association of the two reporter fragments is autoinhibited owing to the thermodynamically favorable interaction of coiled-coils A and B'. Following cleavage of the linker, coiled-coil-mediated complementation of split-protein reporter occurs with concomitant restoration of the reporter activity. The principle of design is shown in Figure 11.^[221] The biorecognition of E/K coiled-coils (E: [EVSALEK]₅; K: [pKVSALKE]₅) was used in the protein detection by western blot^[222] and for the design of a coiled-coil-based ELISA analytical system.^[223] Coiled-coil recognition can be used in specific labeling of proteins in living cells.^[224,225] A peptide probe K3 (KIAALKE)₃ labeled with a fluorophore can specifically stain the surface-exposed tag sequence E3 (EIAALEK)₃ attached to the prostaglandin receptor in living cells.^[224] Similarly, self-assembled protein fibers can be functionalized non-covalently by interaction of two complementary leucine-zipper peptides.^[226]

Yoshida et al. developed self-oscillating hydrogels that can expand and contract without external stimuli. The mechanical oscillation of the gel is caused by dissipating the chemical energy of the oscillating Belousov–Zhabotinsky (BZ) reaction. The catalyst of the BZ reaction, tris(2,2'-bipyridine)ruthenium(II), [Ru(bpy)₃]²⁺, was covalently bound to poly(*N*-isopropylacrylamide) chains within the hydrogel. In a solution containing BZ substrates, the autonomous oxidation (Ru^{III}) and reduction (Ru^{II}) results in changes in hydrogel swelling.^[227–229] Apparently, the chemical energy from the BZ reaction is transduced into the mechanical oscillations of the gels.^[230] To demonstrate the applicability of the design for physiological conditions, Yoshida and Uesasaki synthesized a biomimetic anionic hydrogel (cross-linked copolymer of NIPAAm with 2-methacryloyloxyethyl phosphate) in

which creatine kinase was immobilized, which exhibited self-beating motion in ATP solution, similar to heart muscle. The enzymatic reaction results in changes of calcium ion concentration; as Ca^{2+} chelates (cross-links) phosphoric groups, cross-links are formed and dissociated periodically with concomitant changes in the degree of swelling.^[231] A hydrogel that swells and deswells periodically under constant conditions can be developed in an autonomous mass-transport system.^[232]

A model for biorecognition studies with potential biosensor applications was based on an epitope presentation scaffold, namely an antiparallel coiled-coil heterodimer stem loop (CCSL) peptide self-assembled on a solid substrate. His-tagged CCSL peptides containing peptide epitope sequences, biorecognizable by the CD21 receptor, in the stem loop were designed and synthesized by genetic engineering methods.^[233–235] These peptides self-assembled in the presence of nickel on a polystyrene substrate covalently grafted with an HPMA copolymer containing nitrilotriacetic acid groups. The receptor-binding epitopes were identified by selective binding of Raji B cells and/or soluble CD21 receptor to the self-assembled mono-layer (Figure 12). The efficacy of selected epitopes as targeting moieties in HPMA copolymer–doxorubicin conjugates was evaluated on CD21 positive Raji B cells.^[236]

The surface of poly(acrylamide) hydrogel was functionalized with RGD-containing cell adhesion ligands through self-assembly of a coiled-coil heterodimer.^[237] In a more sophisticated design, coiled-coil-based bioactive surfaces capable of dynamically and reversibly regulating immobilized ligands were produced using a pair of peptides that form heterodimers. Peptide 1 was immobilized to surface by one end, whereas the other end was modified with a cell-adhesive RGD ligand. The complementary peptide 2 was attached to PEG; upon formation of a heterodimer (between peptides 1 and 2), the RGD sequence was shielded by PEG, preventing cell attachment. Addition of an excess of peptide 2 (not conjugated to PEG) resulted in the replacement of peptide 2–PEG conjugate from the surface with concomitant exposure of the RGD ligand.^[238]

Specific biomolecular recognition between coiled-coil-forming sequences was used to assemble gold nanoparticles^[239] or carbon nanotubes.^[240] The use of hydrogel actuators for flow control in drug delivery devices was reviewed by Eddington and Beebe.^[241] Hydrogels may be used as resistance-based valves, jacket valves, electrically triggered valves, and biomimetic valves. The ultimate goal is to enable a physiological feedback to control the infusion rate in a drug-delivery device.

5.5. Formation of Supramolecular Structures Mediated by Biorecognition of Peptide Domains

Biorecognition of coiled-coils can be utilized in programmed assembly of higher-order self-organized systems.^[242] Noncovalent supramolecular assembly of multiple proteins on a dendrimer scaffold resulted in dendrimer-supported fibers with helical secondary structure.^[242] Similarly, formation of an antiparallel leucine zipper directed reassembly of green fluorescent protein (GFP). Two peptide fragments of GFP were modified with coiled-coil-forming peptides; following reassembly, the GFP displayed its characteristic fluorescence.^[243] Chelur and Chalfie demonstrated that co-expression of caspase 3 subunits

generates constitutively active caspase activity (it is active after reconstitution of fragments) that leads to cell death. The caspase activity occurred only when the subunits associated through binding of linked antiparallel coiled-coil domains.^[244] Formation of high-avidity (combined strength of multiple bond interactions) binding molecules has been achieved by coiled-coil recognition. Tetravalent miniantibodies were prepared by self-assembly of four single-chain variable fragment (Fv) fragments connected via a flexible hinge to a tetramerizing helical peptide.^[245] A pentameric multivalent binding molecule (“peptabody”) was formed by self-assembly of a short peptide ligand fused via a semi-rigid hinge region with the coiled-coil assembly domain of the cartilage oligomeric matrix protein.^[246] Diehl et al. used phenylalanine-modified elastin-like peptides to prepare multiunit biomotor assemblies. Cooperative interactions between monomeric kinesin 1 motors attached to protein scaffolds enhanced hydrolytic activity and microtubule gliding velocity.^[247] Recognition of coiled-coil heterodimers was used to assemble noncovalent triblock copolymers, namely PEG–coiled-coil–poly(styrene).^[248] Ryadnov and co-workers designed a cyclo-peptide block consisting of two domains that oligomerize by forming a parallel coiled-coil heterodimer. Self-assembly leads to formation of nano- to micrometer-sized hyperbranched fibrillar networks.^[249]

6. From Nanobiomaterials to Nanomedicine

The self-assembly of hybrid materials, composed of synthetic and biological macromolecules, is mediated by the biorecognition of biological motifs. As discussed above, a pair of oppositely charged pentaheptad peptides (CCE and CCK) that forms antiparallel coiled-coil heterodimers served as physical cross-linkers in self-assembly of HPMA graft copolymers, CCE-P and CCK-P, into hydrogels. It was hypothesized that this unique biorecognition of CCK and CCE peptide motifs could be expanded past biomaterials design and be applied to a living system and mediate a biological process. This would provide a bridge between the designs of biomaterials and macromolecular therapeutics.^[236]

To validate the hypothesis, CCE and CCK were employed in the design of a new apoptosis induction system in CD20 positive cells, called drug free macromolecular therapeutics.^[250,251] CD20 is one of the most reliable biomarkers for B cell non-Hodgkin's lymphoma (NHL); it is a non-internalizing antigen that remains on the cell surface when bound to a complementary antibody. However, cross-linking of CD20-bound antibodies with a secondary antibody results in apoptosis. To exploit this phenomenon, a system composed of CCE and CCK peptides, the Fab' fragment of the 1F5 anti-CD20 antibody, and HPMA copolymer was designed (Figure 13). The exposure of CD20-positive Raji B cells to Fab'-CCE resulted in the decoration of the cell surface with multiple copies of the CCE peptide by antigen–antibody fragment biorecognition. Further exposure of the decorated cells to HPMA copolymer grafted with multiple copies of CCK resulted in the formation of CCE–CCK coiled-coil heterodimers on the cell surface. This second biorecognition event induced cross-linking of CD20 receptors and triggered apoptosis of Raji B cells.^[179] The system was also active in vivo. Intravenous administration of Fab'-CCE conjugate, followed by the administration of CCK-P, produced long-term survivors in SCID (C.B.-17) mice bearing human B-lymphoma xenografts.^[251]

The rationale of the design of drug-free macro-molecular therapeutics is the absence of low-molecular-weight drugs and the fact that cross-linking of CD20 at B-cell surface results in apoptosis. This approach creates a new approach for manipulating molecular recognition principles in the design of improved cancer treatment.

7. Conclusions and Future Prospects

Peptides and proteins provide abundant opportunities to design self-assembling biorecognizable nanomaterials. Most of the current designs are based on ideas drawn from nature. Understanding the principles of protein engineering permits the design of functional proteins and their (future) incorporation into hybrid systems that are novel both in structure and function. Several examples of modern approaches of the management of complexity and utility of protein engineering were recently published. Cornelissen et al. used heterodimeric coiled-coil biorecognition to encapsulate protein (enhanced green fluorescent protein) into a virus (cowpea chlorotic mottle virus) capsid.^[252] Koder et al. designed and synthesized an oxygen transport protein based on the assembly through four stages: assembly of a four-helix bundle, insertion of a cofactor binding amino acid, adjusting the sequence to improve structural resolution, and refining the function.^[253] Tetherin is a coiled-coil-containing protein, the expression of which blocks the release of HIV-1 and other enveloped viral particles from host cells.^[254] Perez-Caballero et al. have shown that tetherin configuration (or structure) rather than primary sequence is critical for its antiviral activity.^[255] They replaced the major domains of tetherin, namely transmembrane, coiled-coil, and glycosylphosphatidylinositol anchor, with analogous motifs from three unrelated proteins,^[255,256] and the fully artificial form of tetherin inhibited particle release, similar to the native molecule (Figure 14).

Peptides, proteins, poly(amino acid)s, and hybrid macro-molecules spontaneously undergo biorecognition-driven self-assembly into precisely defined 3D hydrogel structures. To utilize the wide application potential of these systems, factors that may have an impact on folding and self-assembly need to be identified.^[257–259] Designs that are grounded on solid basic science principles and at the same time find a correlation with biological and technical needs will be translated into practical applications. Developments that may be expected in the near future include: design of hydrogels with multiple functions, hydrogels sensitive to several stimuli, hydrogels with programmable responses, and hydrogels translating substrate recognition into mechanical motion. Further miniaturization of precisely designed hydrogel components of biomedical devices, nanomedicines, sensors, microfluidics systems, nano-reactors, and interactive surfaces with high accuracy of biorecognition are within reach.

Acknowledgments

The research related to this review was supported in part by NIH grants EB005288 and GM095606, and by the University of Utah Research Foundation. We thank Michael Jacobsen for carefully checking the manuscript.

References

1. Kyle S, Aggeli A, Ingham E, McPherson MJ. Trends Biotechnol. 2009; 27:423–433. [PubMed: 19497631]
2. Zhang S. Biotechnol Adv. 2002; 20:321–339. [PubMed: 14550019]

3. Ryadnov MG, Bella A, Timson S, Woolfson DN. *J Am Chem Soc.* 2009; 131:13240–13241. [PubMed: 19708655]
4. Rajagopal K, Schneider JP. *Curr Opin Struct Biol.* 2004; 14:480–486. [PubMed: 15313243]
5. Ikkala O, ten Brinke G. *Chem Commun.* 2004:2131–2137.
6. Matson JB, Stupp SI. *Chem Commun.* 2012; 48:26–33.
7. Cai C, Wang L, Lin J. *Chem Commun.* 2011; 47:11189–11203.
8. Heim M, Römer L, Scheibel T. *Chem Soc Rev.* 2010; 39:156–164. [PubMed: 20023846]
9. Wichterle O, Lím D. *Nature.* 1960; 185:117–118.
10. Kopeček J, Yang J. *Polym Int.* 2007; 56:1078–1098.
11. Kopeček J. *J Polym Sci Part A.* 2009; 47:5929–5946.
12. Kopeček J, Tang A, Wang C, Stewart RJ. *Macromol Symp.* 2001; 174:31–42.
13. Vandermeulen GWM, Klok HA. *Macromol Biosci.* 2004; 4:383–398. [PubMed: 15468229]
14. Kopeček J, Yang J. *Acta Biomater.* 2009; 5:805–816. [PubMed: 18952513]
15. Xu C, Kopeček J. *Polym Bull.* 2007; 58:53–63.
16. Wang C, Varshney RR, Wang DA. *Adv Drug Delivery Rev.* 2010; 62:699–710.
17. Tibbitt MW, Anseth KS. *Biotechnol Bioeng.* 2009; 103:655–663. [PubMed: 19472329]
18. Jia X, Kiick KL. *Macromol Biosci.* 2009; 9:140–156. [PubMed: 19107720]
19. Lin CC, Anseth KS. *Pharm Res.* 2009; 26:631–643. [PubMed: 19089601]
20. Schmidt JJ, Rowley J, Kong HJ. *J Biomed Mater Res Part A.* 2008; 87:1113–1122.
21. Elisseeff J, Ferran A, Hwang S, Varghese S, Zhang Z. *Stem Cells Dev.* 2006; 15:295–303. [PubMed: 16846368]
22. Peppas NA, Hilt JZ, Khademhosseini A, Langer R. *Adv Mater.* 2006; 18:1345–1360.
23. Nayak S, Lyon LA. *Angew Chem.* 2005; 117:7862–7886. *Angew Chem Int Ed.* 2005; 44:7686–7708.
24. Zhu J, Marchant RE. *Expert Rev Med Devices.* 2011; 8:607–626. [PubMed: 22026626]
25. Censi R, Di Martino P, Vermonden T, Hennink WE. *J Controlled Release.* 2012; 161:680–692.
26. Lupas AN, Gruber M. *Adv Protein Chem.* 2005; 70:37–78. [PubMed: 15837513]
27. Woolfson DN. *Adv Protein Chem.* 2005; 70:79–112. [PubMed: 15837514]
28. Parry DA, Fraser RD, Squire JM. *J Struct Biol.* 2008; 163:258–269. [PubMed: 18342539]
29. Moutevelis E, Woolfson DN. *J Mol Biol.* 2009; 385:726–732. [PubMed: 19059267]
30. Su JY, Hodges RS, Kay CM. *Biochemistry.* 1994; 33:15501–15510. [PubMed: 7803412]
31. Oakley MG, Hollenbeck JJ. *Curr Opin Struct Biol.* 2001; 11:450–457. [PubMed: 11495738]
32. Yu B. *Adv Drug Delivery Rev.* 2002; 54:1113–1129.
33. Walshaw J, Woolfson DN. *J Mol Biol.* 2001; 307:1427–1450. [PubMed: 11292353]
34. Gruber M, Lupas AN. *Trends Biochem Sci.* 2003; 28:679–685. [PubMed: 14659700]
35. Woolfson DN, Bartlett GJ, Bruning M, Thomson AR. *Curr Opin Struct Biol.* 2012; 22:1–10. [PubMed: 22265341]
36. Zaccai NR, Chi B, Thomson AR, Boyle AL, Bartlett GJ, Bruning M, Linden N, Sessions RB, Booth PJ, Brady RL, Woolfson DN. *Nat Chem Biol.* 2011; 7:935–941. [PubMed: 22037471]
37. Moll JR, Ruvinov SB, Pastan I, Vinson C. *Protein Sci.* 2001; 10:649–655. [PubMed: 11344333]
38. Singh M, Berger B, Kim PS. *J Mol Biol.* 1999; 290:1031–1041. [PubMed: 10438601]
39. Hodges RS. *Biochem Cell Biol.* 1996; 74:133–154. [PubMed: 9213423]
40. Sia SK, Kim PS. *Biochemistry.* 2001; 40:8981–8989. [PubMed: 11467960]
41. Gerber D, Shai Y. *J Mol Biol.* 2002; 322:491–495. [PubMed: 12225743]
42. Kolluri SK, Zhu X, Zhou X, Lin B, Chen Y, Sun K, Tian X, Town J, Cao X, Lin F, Zhai D, Kitada S, Luciano F, O'Donnell E, Cao Y, He F, Lin J, Reed JC, Satterthwait AC, Zhang XK. *Cancer Cell.* 2008; 14:285–298. [PubMed: 18835031]
43. Welch BD, VanDemark AP, Heroux A, Hill CP, Kay MS. *Proc Natl Acad Sci USA.* 2007; 104:16828–16833. [PubMed: 17942675]

44. Welch BD, Francis JN, Redman JS, Paul S, Weinstein MT, Reeves JD, Lie YS, Whitby FG, Eckert DM, Hill CP, Root MJ, Kay MS. *J Virol.* 2010; 84:11235–11244. [PubMed: 20719956]
45. Funke SA, Willbold D. *Mol BioSyst.* 2009; 5:783–786. [PubMed: 19603110]
46. Pantoja-Uceda D, Santiveri CM, Jiménez MA. *Methods Mol Biol.* 2006; 340:27–51. [PubMed: 16957331]
47. Rughani RV, Salick DA, Lamm MS, Yucler T, Pochan DJ, Schneider JP. *Biomacromolecules.* 2009; 10:1295–1304. [PubMed: 19344123]
48. Davies RPW, Aggeli A. *J Pept Sci.* 2011; 17:107–114. [PubMed: 21234982]
49. Aggeli A, Bell M, Boden N, Keen JN, McLeish TCB, Nyrkova I, Radford SE, Semenov A. *J Mater Chem.* 1997; 7:1135–1145.
50. Chung DM, Nowick JS. *J Am Chem Soc.* 2004; 126:3062–3063. [PubMed: 15012131]
51. Koga T, Matsuoka M, Higashi N. *J Am Chem Soc.* 2005; 127:17596–17597. [PubMed: 16351076]
52. Wiesehan K, Buder K, Linke RP, Patt S, Stoldt M, Unger E, Schmitt B, Bucci E, Willbold D. *ChemBioChem.* 2003; 4:748–753. [PubMed: 12898626]
53. Wiesehan K, Stöhr J, Nager-Steger L, van Groen T, Riesner D, Willbold D. *Protein Eng Des Sel.* 2008; 21:241–246. [PubMed: 18252750]
54. Luo Z, Zhao X, Zhang S. *PLoS ONE.* 2008; 3:e2364. [PubMed: 18509542]
55. Luo Z, Zhao X, Zhang S. *Macromol Biosci.* 2008; 8:785–791. [PubMed: 18546148]
56. Luo Z, Wang S, Zhang S. *Biomaterials.* 2011; 32:2013–2020. [PubMed: 21167593]
57. Altunbas A, Pochan DJ. *Top Curr Chem.* 2012; 310:135–167. [PubMed: 21809190]
58. Schneider JP, Pochan DJ, Ozbas B, Rajagopal K, Pakstis L, Kretsinger J. *J Am Chem Soc.* 2002; 124:15030–15037. [PubMed: 12475347]
59. Ozbas B, Kretsinger J, Rajagopal K, Schneider JP, Pochan DJ. *Macromolecules.* 2004; 37:7331–7337.
60. Haines-Butterick L, Rajagopal K, Branco M, Salick D, Rughani R, Pilarz M, Lamm MS, Pochan DJ, Schneider JP. *Proc Natl Acad Sci USA.* 2007; 104:7791–7796. [PubMed: 17470802]
61. Mason JM, Hagemann UB, Arndt KM. *Biochemistry.* 2009; 48:10380–10388. [PubMed: 19743874]
62. Mason JM, Arndt KM. *ChemBioChem.* 2004; 5:170–176. [PubMed: 14760737]
63. Wang C, Stewart RJ, Kopeček J. *Nature.* 1999; 397:417–420. [PubMed: 9989405]
64. Litowski JR, Hodges RS. *J Biol Chem.* 2002; 277:37272–37279. [PubMed: 12138097]
65. Yu Y, Monera OD, Hodges RS, Privalov PL. *J Mol Biol.* 1996; 255:367–372. [PubMed: 8568882]
66. Zaykov AN, MacKenzie KR, Ball ZT. *Chem Eur J.* 2009; 15:8961–8965. [PubMed: 19637261]
67. Radu LC, Yang J, Kopeček J. *Macromol Biosci.* 2009; 9:36–44. [PubMed: 18855948]
68. Aggeli A, Nyrkova IA, Bell M, Harding R, Carrick L, McLeish TCB, Semenov AN, Boden N. *Proc Natl Acad Sci USA.* 2001; 98:11857–11862. [PubMed: 11592996]
69. Mutter M, Gassmann R, Buttke U, Altmann KH. *Angew Chem.* 1991; 103:1504–1506. *Angew Chem Int Ed Engl.* 1991; 30:1514–1516.
70. Mimna R, Camus MS, Schmid A, Tuchscherer G, Lashuel HA, Mutter M. *Angew Chem.* 2007; 119:2735–2738. *Angew Chem Int Ed.* 2007; 46:2681–2684.
71. Pagel K, Wagner SC, Samedov K, von Berlepsch H, Böttcher C, Kokschi B. *J Am Chem Soc.* 2006; 128:2196–2197. [PubMed: 16478157]
72. Pandya MJ, Cerasoli E, Joseph A, Stoneman RG, Waite E, Woolfson DN. *J Am Chem Soc.* 2004; 126:17016–17024. [PubMed: 15612740]
73. Pagel K, Vagt T, Kohajda T, Kokschi B. *Org Biomol Chem.* 2005; 3:2500–2502. [PubMed: 15999178]
74. Pechar M, Kopeckova P, Joss L, Kopeček J. *Macromol Biosci.* 2002; 2:199–206.
75. Vandermeulen GWM, Tziatzios C, Klok HA. *Macromolecules.* 2003; 36:4107–4114.
76. Castelletto V, Newby GE, Zhu Z, Hamley IW, Noirez L. *Langmuir.* 2010; 26:9986–9996. [PubMed: 20450168]

77. Grieshaber SE, Nie T, Yan C, Zhong S, Teller SS, Clifton RJ, Pochan DJ, Kiick KL, Jia X. *Macromol Chem Phys*. 2011; 212:229–239. [PubMed: 21359141]
78. Top A, Roberts CJ, Kiick KL. *Biomacromolecules*. 2011; 12:2184–2192. [PubMed: 21553871]
79. Tae G, Kornfeld JA, Hubbell JA. *Biomaterials*. 2005; 26:5259–5266. [PubMed: 15792553]
80. Quémener D, Deratani A, Lecommandoux S. *Top Curr Chem*. 2012; 322:165–192. [PubMed: 22025063]
81. Pechar M, Pola R. *Biotech Adv*. 201210.1016/j.biotechadv.2012.01.003
82. Kopeček J. *Biomaterials*. 2007; 28:5185–5192. [PubMed: 17697712]
83. Ulijn RV, Smith AM. *Chem Soc Rev*. 2008; 37:664–675. [PubMed: 18362975]
84. Petka WA, Harden JL, McGrath KP, Wirtz D, Tirrell DA. *Science*. 1998; 281:389–392. [PubMed: 9665877]
85. Xu C, Breedveld V, Kopeček J. *Biomacromolecules*. 2005; 6:1739–1749. [PubMed: 15877401]
86. Wang C, Kopeček J, Stewart RJ. *Biomacromolecules*. 2001; 2:912–920. [PubMed: 11710049]
87. Chen L, Kopeček J, Stewart RJ. *Bioconjugate Chem*. 2000; 11:734–740.
88. Apostolovic B, Danial M, Klok HA. *Chem Soc Rev*. 2010; 39:3541–3575. [PubMed: 20676430]
89. Sadownik JW, Ulijn RV. *Curr Opin Biotechnol*. 2010; 21:401–411. [PubMed: 20594820]
90. Robson Mardsen H, Kros A. *Angew Chem*. 2010; 122:3050–3068. *Angew Chem Int Ed*. 2010; 49:2988–3005.
91. Collier JH, Segura T. *Biomaterials*. 2011; 32:4198–4204. [PubMed: 21515167]
92. Doel MT, Eaton M, Cook EA, Lewis H, Patel T, Carrey NH. *Nucleic Acids Res*. 1980; 8:4575–4592. [PubMed: 7003541]
93. Cappello J. *Trends Biotechnol*. 1990; 8:309–311. [PubMed: 1366767]
94. Cappello, J. *Handbook of Biodegradable Polymers*. Domb, AJ.; Kost, J.; Wiseman, DM., editors. Harwood Academic Publishers; Amsterdam: 1997. p. 387-416.
95. Ghandehari H, Capello J. *Pharm Res*. 1998; 15:813–815. [PubMed: 9647343]
96. Dinerman AA, Capello J, Ghandehari H, Hoag SW. *Biomaterials*. 2002; 23:4203–4210. [PubMed: 12194523]
97. Dinerman AA, Capello J, Ghandehari H, Hoag SW. *J Controlled Release*. 2002; 82:277–287.
98. Megeed Z, Capello J, Ghandehari H. *Pharm Res*. 2002; 19:954–959. [PubMed: 12180547]
99. Nagarsekar A, Crissman J, Crissman M, Ferrari F, Capello J, Ghandehari H. *J Biomed Mater Res*. 2002; 62:195–203. [PubMed: 12209939]
100. Nagarsekar A, Crissman J, Crissman M, Ferrari F, Capello J, Ghandehari H. *Biomacromolecules*. 2003; 4:602–607. [PubMed: 12741775]
101. Haider M, Leung V, Ferrari F, Crissman J, Powell J, Capello J, Ghandehari H. *Mol Pharm*. 2005; 2:139–150. [PubMed: 15804188]
102. Hwang D, Moolchandani V, Dandu R, Haider M, Capello J, Ghandehari H. *Int J Pharm*. 2009; 368:215–219. [PubMed: 19027056]
103. Greish K, Araki K, Li D, O'Malley BW Jr, Dandu R, Frandsen J, Capello J, Ghandehari H. *Biomacromolecules*. 2009; 10:2183–2188. [PubMed: 19722557]
104. Hwang W, Kim BH, Dandu R, Capello J, Ghandehari H, Seong J. *Langmuir*. 2009; 25:12682–12686. [PubMed: 19803470]
105. Urry DW. *Angew Chem*. 1993; 105:859–883. *Angew Chem Int Ed Engl*. 1993; 32:819–841.
106. Urry DW. *Trends Biotechnol*. 1999; 17:249–257. [PubMed: 10354563]
107. Wright ER, McMillan RA, Cooper A, Apkarian RP, Conticello VP. *Adv Funct Mater*. 2002; 12:149–154.
108. Wu X, Sallach RE, Caves JM, Conticello VP, Chaikof EL. *Biomacromolecules*. 2008; 9:1787–1794. [PubMed: 18558738]
109. Creel HS, Founier MJ, Mason TL, Tirrell DA. *Macro-molecules*. 1991; 24:1213–1214.
110. McGrath KP, Founier MJ, Mason TL, Tirrell DA. *J Am Chem Soc*. 1992; 114:727–733.
111. Krejchi MT, Atkins EDT, Waddon AJ, Founier MJ, Mason TL, Tirrell DA. *Science*. 1994; 265:1427–1432. [PubMed: 8073284]

112. Xu C, Kopeček J. *Pharm Res.* 2008; 25:674–682. [PubMed: 17713844]
113. Shen, W. PhD Thesis. California Institute of Technology; Pasadena: 2005.
114. Shen W, Kornfeld JA, Tirrell DA. *Soft Mater.* 2007; 3:99–107.
115. Shen W, Zhang K, Kornfeld JA, Tirrell DA. *Nat Mater.* 2006; 5:153–158. [PubMed: 16444261]
116. Macias MJ, Gervais V, Civera C, Oschkinat H. *Nat Struct Biol.* 2000; 7:375–379. [PubMed: 10802733]
117. Wong Po Foo CTS, Lee JS, Mulyasmita W, Parisi-Amon A, Heilshorn SC. *Proc Natl Acad Sci USA.* 2009; 106:22067–22072. [PubMed: 20007785]
118. Mulyasmita W, Lee JS, Heilshorn SC. *Biomacromolecules.* 2011; 12:3406–3411. [PubMed: 21861461]
119. Nowak AP, Breedveld V, Pakstis L, Ozbas B, Pine DJ, Pochan D, Deming TJ. *Nature.* 2002; 417:424–428. [PubMed: 12024209]
120. Breedveld V, Nowak AP, Sato J, Deming TJ, Pine DJ. *Macromolecules.* 2004; 37:3943–3953.
121. Nowak AP, Sato J, Breedveld V, Deming TJ. *Supramol Chem.* 2006; 18:423–427.
122. Deming TJ. *Soft Matter.* 2005; 1:28–35.
123. Kopeček J. *Nature.* 2002; 417:388–391. [PubMed: 12024197]
124. Madsen HR, Handgraaf JW, Nudelman F, Sommerdijk NAJM, Kros A. *J Am Chem Soc.* 2010; 132:2370–2377. [PubMed: 20108940]
125. Elvin CM, Carr AG, Huson MG, Maxwell JM, Pearson RD, Vuocolo T, Liyou NE, Wong DC, Merritt DJ, Dixon NE. *Nature.* 2005; 437:999–1002. [PubMed: 16222249]
126. Lv S, Dudek DM, Cao Y, Balamurali MM, Gosline J, Li H. *Nature.* 2010; 465:69–73. [PubMed: 20445626]
127. Cao Y, Li H. *Chem Commun.* 2008:4144–4146.
128. Yang J, Xu C, Wang C, Kopeček J. *Biomacromolecules.* 2006; 7:1187–1195. [PubMed: 16602737]
129. Lv S, Cao Y, Li H. *Langmuir.* 2012; 28:2269–2274. [PubMed: 22085110]
130. Chen JS, Altman GH, Karageorgiou V, Horan R, Collette A, Volloch V, Colabro T, Kaplan DL. *J Biomed Mater Res Part A.* 2003; 67:559–570.
131. Urry DW, Pattanaik A, Xu J, Woods TC, McPherson DT, Parker TM. *J Biomater Sci Polym Ed.* 1998; 9:1015–1048. [PubMed: 9806444]
132. Kobatake E, Onoda K, Yanagida Y, Aizawa M. *Biomacromolecules.* 2000; 1:382–386. [PubMed: 11710127]
133. Liu JC, Heilshorn SC, Tirrell DA. *Biomacromolecules.* 2004; 5:497–504. [PubMed: 15003012]
134. Mi L, Fischer S, Chung B, Sundelacruz S, Harden JL. *Biomacromolecules.* 2006; 7:38–47. [PubMed: 16398496]
135. Kumar M, Sanford KJ, Cuevas WP, Du M, Collier KD, Chow N. *Biomacromolecules.* 2006; 7:2543–2551. [PubMed: 16961316]
136. Gomes SC, Leonor IB, Mano JF, Reis RL, Kaplan DL. *Biomaterials.* 2011; 32:4255–4266. [PubMed: 21458065]
137. Kopeček J, Wang C, Stewart R. *Abstr Pap Am Chem Soc.* 1998; 216:U56–U57.
138. Ulbrich K, Strohalm J, Kopeček J. *Biomaterials.* 1982; 3:150–154. [PubMed: 7115858]
139. Rejmanová P, Pohl J, Baudyš M, Kostka V, Kopeček J. *Makromol Chem.* 1983; 184:2009–2020.
140. Šubr V, Duncan R, Kopeček J. *J Biomater Sci Polym Ed.* 1990; 1:261–278. [PubMed: 1703786]
141. Miyata T, Asami T, Urugami T. *Nature.* 1999; 399:766–769. [PubMed: 10391240]
142. Lu ZR, Kopečková P, Kopeček J. *Macromol Biosci.* 2003; 3:296–300.
143. Hu BH, Messersmith PB. *J Am Chem Soc.* 2003; 125:14298–14299. [PubMed: 14624577]
144. Jing P, Rudra JS, Herr AB, Collier JH. *Biomacromolecules.* 2008; 9:2438–2446. [PubMed: 18712921]
145. Sahin E, Kiick KL. *Biomacromolecules.* 2009; 10:2740–2749. [PubMed: 19743840]
146. Rubert Pérez CM, Panitch A, Chmielewski J. *Macromol Biosci.* 2011; 11:1426–1431. [PubMed: 21830301]

147. Yang J, Wu K, Kopeček J, Kopeček J. *Biomacromolecules*. 2008; 9:510–517. [PubMed: 18208316]
148. McClain DL, Woods HL, Oakley MG. *J Am Chem Soc*. 2001; 123:3151–3152. [PubMed: 11457033]
149. See Ref. [31].
150. Oakley MG, Kim PS. *Biochemistry*. 1998; 37:12603–12610. [PubMed: 9730833]
151. Radu-Wu L, Yang J, Wu K, Kopeček J. *Biomacromolecules*. 2009; 10:2319–2327. [PubMed: 19591463]
152. Wu L, Yang J, Kopeček J. *Biomaterials*. 2011; 32:5341–5353. [PubMed: 21549421]
153. Dušek K, Dušková-Smrková M, Stewart R, Kopeček J. *Polym Bull*. 2001; 47:351–358.
154. Hamley IW, Ansari IA, Castelletto V, Nuhn H, Rösler A, Klok HA. *Biomacromolecules*. 2005; 6:1310–1315. [PubMed: 15877346]
155. Rösler A, Klok HA, Hamley IW, Castelletto V, Mykhaylyk OO. *Biomacromolecules*. 2003; 4:859–863. [PubMed: 12857065]
156. Burkoth TS, Benzinger TLS, Jones DNM, Hallenga K, Meredith SC, Lynn DG. *J Am Chem Soc*. 1998; 120:7655–7656.
157. Burkoth TS, Benzinger TLS, Urban V, Lynn DG, Meredith SC, Thiyagarajan P. *J Am Chem Soc*. 1999; 121:7429–7430.
158. Burkoth TS, Benzinger TLS, Urban V, Morgan DM, Gregory DM, Thiyagarajan P, Botto RE, Meredith SC, Lynn DG. *J Am Chem Soc*. 2000; 122:7883–7889.
159. Hentschel J, Krause E, Börner HG. *J Am Chem Soc*. 2006; 128:7722–7723. [PubMed: 16771470]
160. Pechar M, Brus J, Kostka L, Kopeček J, Urbanová M, Šlouf M. *Macromol Biosci*. 2007; 7:56–69. [PubMed: 17238231]
161. Ehrick JD, Deo SK, Browning TW, Bachas LG, Madou MJ, Daunert S. *Nat Mater*. 2005; 4:298–302. [PubMed: 15765106]
162. Murphy WL, Dillmore WS, Modica J, Mrksich M. *Angew Chem*. 2007; 119:3126–3129. *Angew Chem Int Ed*. 2007; 46:3066–3069.
163. Sui Z, King WJ, Murphy WL. *Adv Mater*. 2007; 19:3377–3380.
164. Ehrick JD, Luckett MR, Khatwani S, Wei Y, Deo SK, Bachas LG, Daunert S. *Macromol Biosci*. 2009; 9:864–868. [PubMed: 19434674]
165. Yuan W, Yang J, Kopečková P, Kopeček J. *J Am Chem Soc*. 2008; 130:15760–15761. [PubMed: 18980321]
166. Jacob MH, Amir D, Ratner V, Gussakowsky E, Haas E. *Biochemistry*. 2005; 44:13664–13672. [PubMed: 16229456]
167. Kennedy SB, deAzevedo ER, Petka WA, Russell TP, Tirrell DA, Hong M. *Macromolecules*. 2001; 34:8675–8685.
168. Hong M, Isailovic D, McMillan RA, Conticello VP. *Biopolymers*. 2003; 70:158–168. [PubMed: 14517905]
169. Kurková D, Kříž J, Schmidt P, Dybal J, Rodríguez-Cabello JC, Alonso M. *Biomacromolecules*. 2003; 4:589–601. [PubMed: 12741774]
170. Lindhout DA, Litkowski JR, Mercier P, Hodges RS, Sykes BD. *Biopolymers*. 2004; 75:367–375. [PubMed: 15457434]
171. Pagel K, Seeger K, Seiwert B, Villaq A, Mark AE, Berger S, Kokscha B. *Org Biomol Chem*. 2005; 3:1189–1194. [PubMed: 15785806]
172. Dušek K, Dušková-Smrková M, Yang J, Kopeček J. *Macromolecules*. 2009; 42:2265–2274. [PubMed: 20160932]
173. Fang L, Brown W, Kopeček J. *Macromolecules*. 1991; 24:6839–6842.
174. Kopeček J, Kopečková P, Kopeček J. *Macromolecules*. 1992; 25:5451–5456.
175. Nie H, Li M, Bansil R, Kopeček J, Helmstedt M, Lal J. *Polymer*. 2004; 45:8791–8799.
176. Mason TG, Gang H, Weitz DA. *J Opt Soc Am A*. 1997; 14:139–149.
177. Mason TG, Weitz DA. *Phys Rev Lett*. 1995; 74:1250–1253. [PubMed: 10058972]

178. Crocker JC, Valentine MT, Weeks ER, Gisler T, Kaplan PD, Yodanis CL, Weitz DA. *Phys Rev Lett*. 2000; 85:888–891. [PubMed: 10991424]
179. Larsen TH, Furst EM. *Phys Rev Lett*. 2008; 100:146001. [PubMed: 18518051]
180. Yang J, Xu C, Kopeček P, Kopeček J. *Macromol Biosci*. 2006; 6:201–209. [PubMed: 16514591]
181. Wu K, Yang J, Kopeček P, Kopeček J. *Macromol Chem Phys*. 2008; 209:467–475.
182. Shibayama M. *Polym J*. 2011; 43:18–34. and references therein.
183. Zizlsperger N, Malashkevich VN, Pillay S, Keating AE. *Biochemistry*. 2008; 47:11858–11868. [PubMed: 18850724]
184. Salwiczek M, Samsonov S, Vagt T, Nyakatura E, Fleige E, Numata J, Cölfen H, Pisabarro MT, Kokscha B. *Chem Eur J*. 2009; 15:7628–7636. [PubMed: 19579235]
185. Eisenhawer M, Cattarinussi S, Kuhn A, Vogel H. *Biochemistry*. 2001; 40:12321–12328. [PubMed: 11591151]
186. Maskarinec SA, Tirrell DA. *Curr Opin Biotechnol*. 2005; 16:422–426. [PubMed: 16006115]
187. Lutolf MP, Gilbert PM, Blau HM. *Nature*. 2009; 462:433–441. [PubMed: 19940913]
188. Discher DE, Mooney DJ, Zandstra PW. *Science*. 2009; 324:1673–1677. [PubMed: 19556500]
189. Lee SH, Moon JJ, West JL. *Biomaterials*. 2008; 29:2962–2968. [PubMed: 18433863]
190. Šprinc L, Kopeček J, Lím D. *Calc Tiss Res*. 1973; 13:63–72.
191. Engler AJ, Sen S, Sweeney HL, Discher DE. *Cell*. 2006; 126:677–689. [PubMed: 16923388]
192. Lutolf MP, Hubbell JA. *Nat Biotechnol*. 2005; 23:47–55. [PubMed: 15637621]
193. Lutolf MP, Lauer-Fields JL, Schmoekel HG, Metters AT, Weber FE, Fields GB, Hubbell JA. *Proc Natl Acad Sci USA*. 2003; 100:5413–5418. [PubMed: 12686696]
194. Petersen OW, Rønnow-Jessen L, Howlett AR, Bissell MJ. *Proc Natl Acad Sci USA*. 1992; 89:9064–9068. [PubMed: 1384042]
195. Lee KY, Alsberg E, Hsiong S, Comisar W, Linderman J, Ziff R, Mooney D. *Nano Lett*. 2004; 4:1501–1506. [PubMed: 25067913]
196. Kloxin AM, Benton JA, Anseth KS. *Biomaterials*. 2010; 31:1–8. [PubMed: 19788947]
197. Haider M, Cappello J, Ghandehari H, Leong KW. *Pharm Res*. 2008; 25:692–699. [PubMed: 17404809]
198. Megeed Z, Haider M, Li D, O'Malley BW Jr, Cappello J, Ghandehari H. *J Controlled Release*. 2004; 94:433–445.
199. Cresce AV, Dandu R, Burger A, Cappello J, Ghandehari H. *Mol Pharm*. 2008; 5:891–897. [PubMed: 18763804]
200. Gustafson J, Greish K, Frandsen J, Cappello J, Ghandehari H. *J Controlled Release*. 2009; 140:256–261.
201. Gustafson JA, Price RA, Greish K, Cappello J, Ghandehari H. *Mol Pharm*. 2010; 7:1050–1056. [PubMed: 20586469]
202. Gustafson JA, Ghandehari H. *Adv Drug Delivery Rev*. 2010; 62:1509–1523.
203. Branco MC, Pochan DJ, Wagner NJ, Schneider JP. *Biomaterials*. 2010; 31:9527–9534. [PubMed: 20952055]
204. King WJ, Mohammed JS, Murphy WL. *Soft Matter*. 2009; 5:2399–2406.
205. King WJ, Pytel NJ, Ng K, Murphy WL. *Macromol Biosci*. 2010; 10:580–584. [PubMed: 20127670]
206. Ehrbar M, Schoenmakers R, Christen EH, Fussenegger M, Weber W. *Nat Mater*. 2008; 7:800–804. commentary: C. Alexander, *Nat. Mater.* **2008**, 7, 767. [PubMed: 18690239]
207. Yamaguchi N, Zhang L, Chae BS, Palla CS, Furst EM, Kiick KL. *J Am Chem Soc*. 2007; 129:3040–3041. [PubMed: 17315874]
208. Pechar M, Pola R, Laga R, Ulbrich K, Bednarová L, Malo P, Siegllová I, Král V, Fabry M, Vaněk O. *Biomacromolecules*. 2011; 12:3645–3655. [PubMed: 21863890]
209. Apostolovic B, Deacon SPE, Duncan R, Klok HA. *Macromol Rapid Commun*. 2011; 32:11–18. [PubMed: 21432965]

210. Apostolovic B, Deacon SPE, Duncan R, Klok HA. *Biomacromolecules*. 2010; 11:1187–1195. [PubMed: 20359192]
211. Deacon SPE, Apostolovic B, Carbajo RJ, Schott AK, Beck K, Vicent MJ, Pineda-Lucena A, Klok HA, Duncan R. *Biomacromolecules*. 2011; 12:19–27. [PubMed: 21141810]
212. Varghese S, Elisseeff JH. *Adv Polym Sci*. 2006; 203:95–144.
213. Yasuda K, Kitamura N, Gong JP, Arakaki K, Kwon HJ, Onodera S, Chen YM, Kurokawa T, Kanaya F, Ohmiya Y, Osada Y. *Macromol Biosci*. 2009; 9:307–316. [PubMed: 19031389]
214. Semino CE. *J Dent Res*. 2008; 87:606–16. [PubMed: 18573978]
215. Shah RN, Shah NA, Del Rosario Lim MM, Hsieh C, Nuber G, Stupp SI. *Proc Natl Acad Sci USA*. 2010; 107:3293–3298. [PubMed: 20133666]
216. Betre H, Seton LA, Meyer DE, Chilkoti A. *Biomacromolecules*. 2002; 3:910–916. [PubMed: 12217035]
217. Hartgerink JD, Beniash E, Stupp SI. *Science*. 2001; 294:1684–1688. [PubMed: 11721046]
218. Segman-Magidovich S, Grisaru H, Gitli T, Levi-Kalisman Y, Rapaport H. *Adv Mater*. 2008; 20:2156–2161.
219. Gungormus M, Branco M, Fong H, Schneider JP, Tamerler C, Sarikaya M. *Biomaterials*. 2010; 31:7266–7274. [PubMed: 20591477]
220. Gungormus M, Fong H, Kim IW, Evans JS, Tamerler C, Sarikaya M. *Biomacromolecules*. 2008; 9:966–973. [PubMed: 18271563]
221. Shekhawat SS, Porter JR, Sriprasad A, Ghosh I. *J Am Chem Soc*. 2009; 131:15284–15290. [PubMed: 19803505]
222. Boucher C, St-Laurent G, Jolicœur M, De Crescenzo G, Durocher Y. *Anal Biochem*. 2010; 399:138–140. [PubMed: 20005863]
223. Liberelle B, Bartholin L, Boucher C, Murschel F, Jolicœur M, Durocher Y, Merzouki A, De Crescenzo G. *J Immunol Methods*. 2010; 362:161–167. [PubMed: 20869967]
224. Yano Y, Yano A, Oishi S, Sugimoto Y, Tsujimoto G, Fujii N, Matsuzaki K. *ACS Chem Biol*. 2008; 3:341–345. [PubMed: 18533657]
225. Yano Y, Kawano K, Omae K, Matsuzaki K. *Methods Enzymol*. 2012; 504:355–370. [PubMed: 22264544]
226. Mahmoud ZH, Grundy DJ, Channon KJ, Woolfson DN. *Biomaterials*. 2010; 31:7468–7474. [PubMed: 20638122]
227. Yoshida R, Takahashi T, Yamaguchi T, Ichijo H. *J Am Chem Soc*. 1996; 118:5134–5135.
228. Yoshida R, Takei K, Yamaguchi T. *Macromolecules*. 2003; 36:1759–1761.
229. Tateyama S, Shibuta Y, Yoshida R. *J Phys Chem B*. 2008; 112:1777–1782. [PubMed: 18205351]
230. Yashin VV, Kuksenok O, Balasz AC. *Prog Polym Sci*. 2010; 35:155–173.
231. Yoshida R, Uesusuki Y. *Biomacromolecules*. 2005; 6:2923–2926. [PubMed: 16283708]
232. Murase Y, Takeshima R, Yoshida R. *Macromol Biosci*. 2011; 11:1713–1721. [PubMed: 21919207]
233. Tang A, Wang C, Stewart R, Kopeček J. *Bioconjugate Chem*. 2000; 11:363–371.
234. Tang A, Wang C, Stewart RJ, Kopeček J. *J Controlled Release*. 2001; 72:57–70.
235. Tang A, Kopeček J. *Biomacromolecules*. 2002; 3:421–431. [PubMed: 12005510]
236. Tang A, Kopečková P, Kopeček J. *Pharm Res*. 2003; 20:360–367. [PubMed: 12669954]
237. Wilcox PJ, Reinhart-King CA, Lahr SJ, DeGrado WF, Hammer DA. *Biomaterials*. 2005; 26:4757–4766. [PubMed: 15763255]
238. Liu B, Liu Y, Riesberg JJ, Shen W. *J Am Chem Soc*. 2010; 132:13630–13632. [PubMed: 20839864]
239. Stevens MM, Flynn NT, Wang C, Tirrell DA, Langer R. *Adv Mater*. 2004; 16:915–918.
240. Contarino MR, Sergi M, Harrington AE, Lazareck A, Xu J, Chaiken I. *J Mol Recognit*. 2006; 19:363–371. [PubMed: 16775846]
241. Eddington DT, Beebe DJ. *Adv Drug Delivery Rev*. 2004; 56:199–210.
242. Zhou M, Bentley D, Ghosh I. *J Am Chem Soc*. 2004; 126:734–735. [PubMed: 14733545]

243. Ghosh I, Hamilton AD, Regan L. *J Am Chem Soc.* 2000; 122:5658–5659.
244. Chelur DS, Chalfie M. *Proc Natl Acad Sci USA.* 2007; 104:2283–2288. [PubMed: 17283333]
245. Pack P, Müller K, Zahn R, Plückthun A. *J Mol Biol.* 1995; 246:28–34. [PubMed: 7853401]
246. Terskikh AV, Le Doussal JM, Crameri R, Fisch I, Mach JP, Kajava AV. *Proc Natl Acad Sci USA.* 1997; 94:1663–1668. [PubMed: 9050835]
247. Diehl MR, Zhang K, Lee HJ, Tirrell DA. *Science.* 2006; 311:1468–1471. [PubMed: 16527982]
248. Marsden HR, Korobko AV, van Leeuwen ENM, Pouget EM, Veen SJ, Sommerdijk NAJM, Kros A. *J Am Chem Soc.* 2008; 130:9386–9393. [PubMed: 18582047]
249. Bella A, Ray S, Shaw M, Ryadnov MG. *Angew Chem.* 2012; 124:443–446. *Angew Chem Int Ed.* 2012; 51:428–431.
250. Wu K, Liu J, Johnson RN, Yang J, Kopeček J. *Angew Chem.* 2010; 122:1493–1497. *Angew Chem Int Ed.* 2010; 49:1451–1455.
251. Wu K, Yang J, Liu J, Kopeček J. *J Controlled Release.* 2012; 157:126–131.
252. Minten IJ, Hendriks LJA, Nolte RJM, Cornelissen JJLM. *J Am Chem Soc.* 2009; 131:17771–17773. [PubMed: 19995072]
253. Koder RL, Anderson JLR, Solomon LA, Reddy KS, Moser CC, Dutton PL. *Nature.* 2009; 458:305–309. [PubMed: 19295603]
254. Neil SJ, Zang T, Bieniasz PD. *Nature.* 2008; 451:425–430. [PubMed: 18200009]
255. Perez-Caballero D, Zang T, Ebrahimi A, McNatt MW, Gregory DA, Johnson MC, Bieniasz PD. *Cell.* 2009; 139:499–511. [PubMed: 19879838]
256. Hammonds J, Spearman P. *Cell.* 2009; 139:456–457. [PubMed: 19879831]
257. Wagner SC, Roskamp M, Pallerla M, Araghi RR, Schlecht S, Kokscha B. *Small.* 2010; 6:1321–1328. [PubMed: 20517875]
258. Reinke AW, Grant RA, Keating AE. *J Am Chem Soc.* 2010; 132:6025–6031. [PubMed: 20387835]
259. Yang Y, Ringler P, Müller SA, Burkhard P. *J Struct Biol.* 2012; 177:168–176. [PubMed: 22115997]

Biographies



Jindřich (Henry) Kopeček received his Ph.D. in Macromolecular Chemistry and D.Sc. in Chemistry from the Czechoslovak Academy of Sciences. His postdoctoral studies were carried out at the National Research Council of Canada. He is currently Distinguished Professor of Pharmaceutical Chemistry and Distinguished Professor of Bioengineering at the University of Utah. His research focuses on biorecognition of macromolecules, bioconjugate chemistry, targetable macromolecular therapeutics, and the self-assembly of block and graft copolymers into hybrid hydrogels.



Jiyuan (Jane) Yang received her B.S. degree in Chemical Engineering from Tsinghua University, M.S. in Polymer Materials from Dalian University of Technology, and Ph.D. in Biomedical Polymer Science from Peking University. After postdoctoral studies at the Institute Curie in Paris, she joined the University of Utah in 2003. She is currently Research Associate Professor of Pharmaceutics and Pharmaceutical Chemistry. Her research focuses on the design of backbone-degradable, long-circulating polymeric anticancer drug carriers and on the self-assembly of block and graft copolymers into hydrogels mediated by the biorecognition of peptide domains.

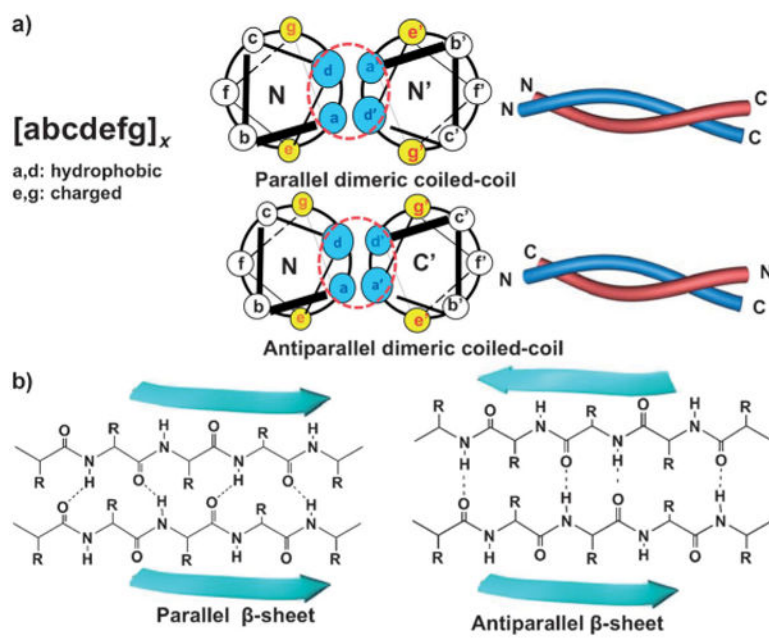


Figure 1.
 Structure of coiled-coils (a) and β -sheets (b).

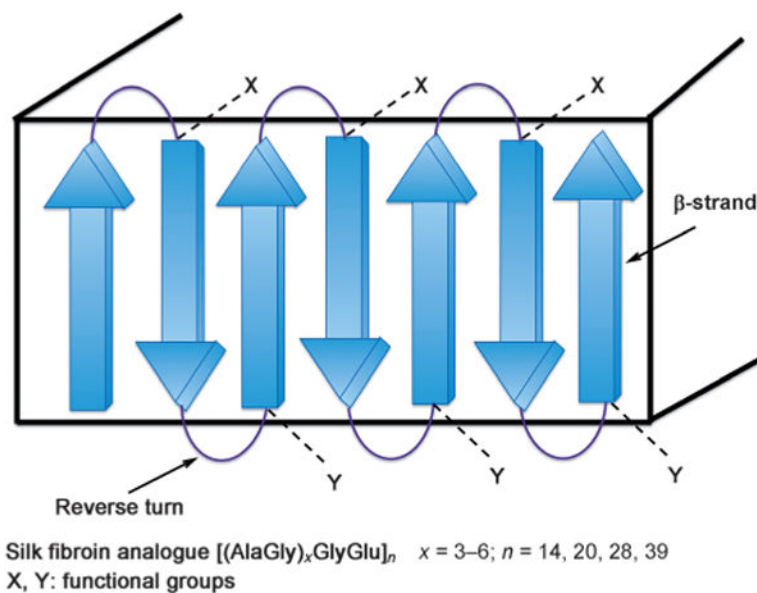


Figure 2. The design and synthesis of architecturally well-defined polypeptides. The surface of the solid structure is decorated in a predetermined pattern with functional groups. Adapted from Ref. [111].

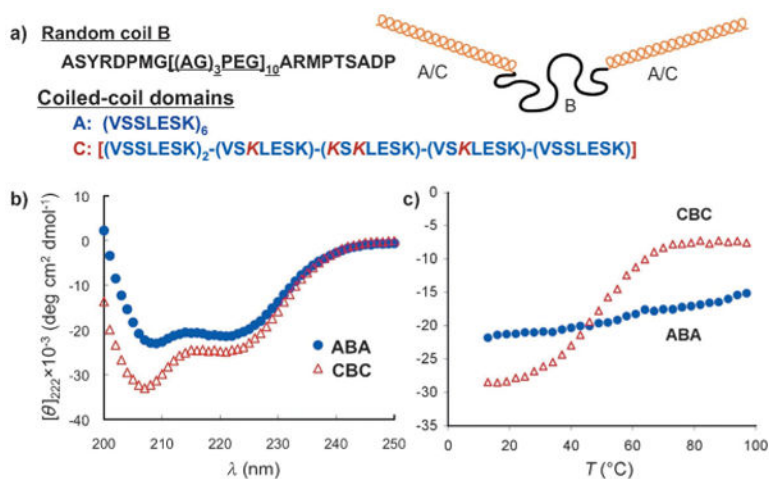


Figure 3.

Temperature dependence of the secondary structure of genetically engineered protein ABA and CBC triblock copolymers. a) Structure of blocks A, B, and C. b) CD signal (ellipticity) as a function of wavelength. c) CD signal at 222 nm as a function of temperature. Minor changes in the coiled-coil block structure results in dramatic changes in stability (structure A changed to structure C, where K replaced V in the a position of the fourth heptad, and three additional K residues replaced S in the c positions of the third, fourth, and the fifth heptad; the random coil block B was without change). Adapted from Ref. [85].

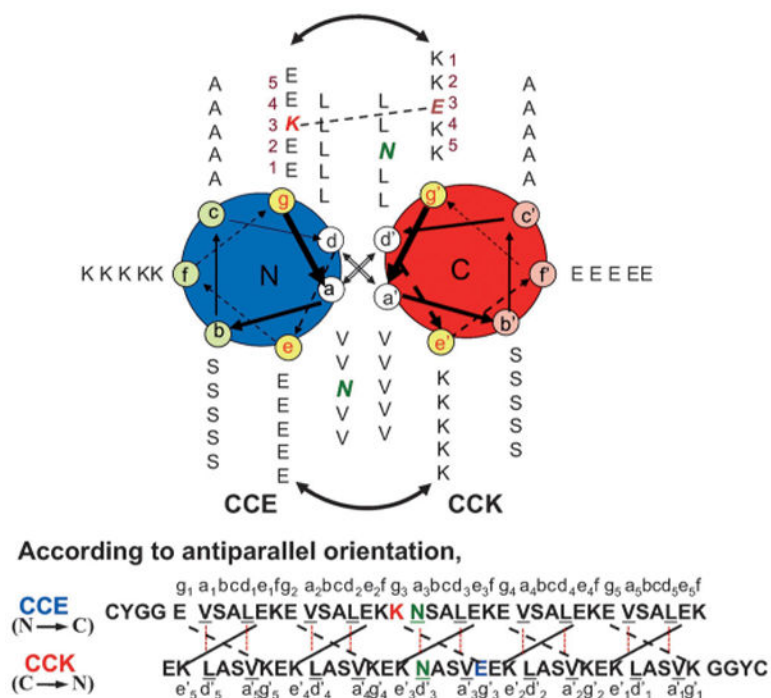
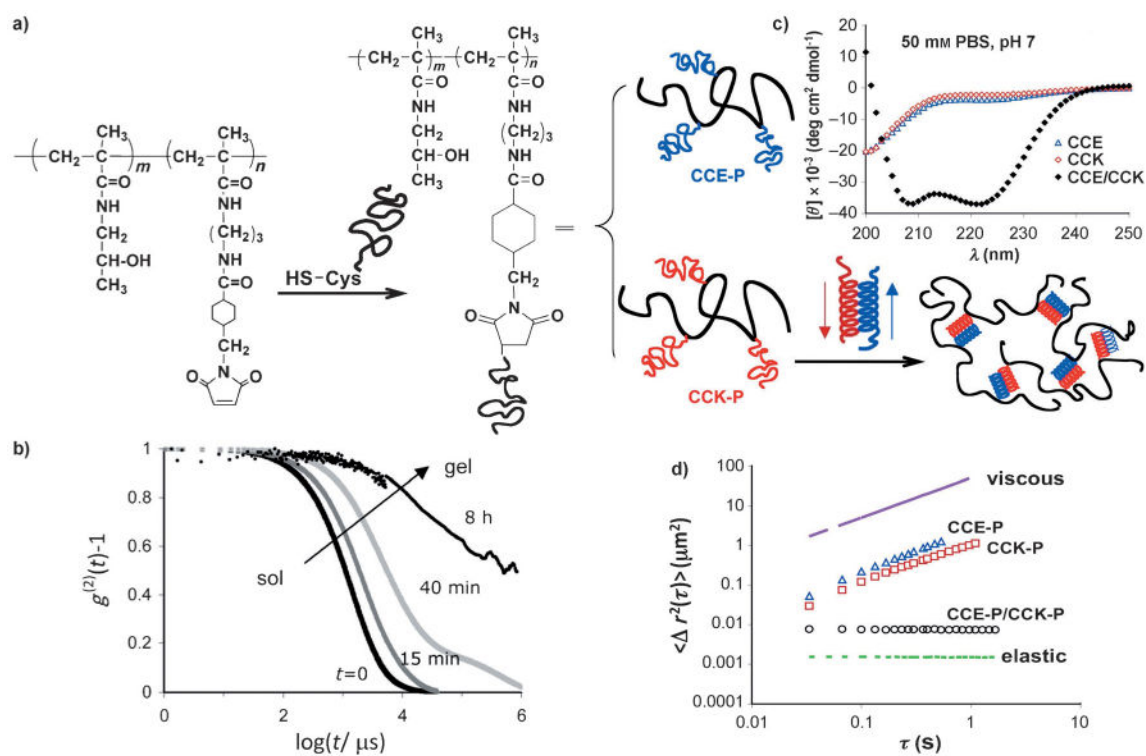


Figure 4.

Helical wheel representation of two-stranded, antiparallel α -helical coiled-coils formed by the dimerization of CCE and CCK. The view is shown looking down the superhelical axis from the N-terminus of CCE and from the C-terminus of CCK. CC denotes the coiled-coil peptides. E and K denote peptides in which most of the e and g positions are occupied by either glutamic acid or lysine, respectively. The sequences are written in the one-letter amino acid code. Positions a and d of the heptad repeat are underlined and form the hydrophobic core of the coiled-coil. Adapted from Ref. [128].

**Figure 5.**

a) Self-assembly of HPMA graft copolymers, CCE-P and CCK-P, containing oppositely charged peptide grafts (P is the HPMA copolymer backbone). Aqueous solutions of CCE-P or CCK-P did not form hydrogels. In contrast, gel-like materials were formed from equimolar mixtures of CCE-P/CCK-P at low concentrations. b) Normalized intensity autocorrelation functions, $g^{(2)}(t)-1$, for solutions (equimolar mixtures) of CCE-P and CCK-P (total concentration 10 mg mL^{-1}) at different incubation times: immediately after mixing, 15 min, 40 min, and 8 h after mixing. c) CD spectra of CCE, CCK, and equimolar mixture CCE/CCK. PBS = phosphate-buffered saline. d) Microrheology of 1 % w/v solutions of CCE-P, CCK-P, and an equimolar mixture of CCE-P/CCK-P. Mean square displacement of tracking particles is a function of time. Adapted from Refs. [128, 147].

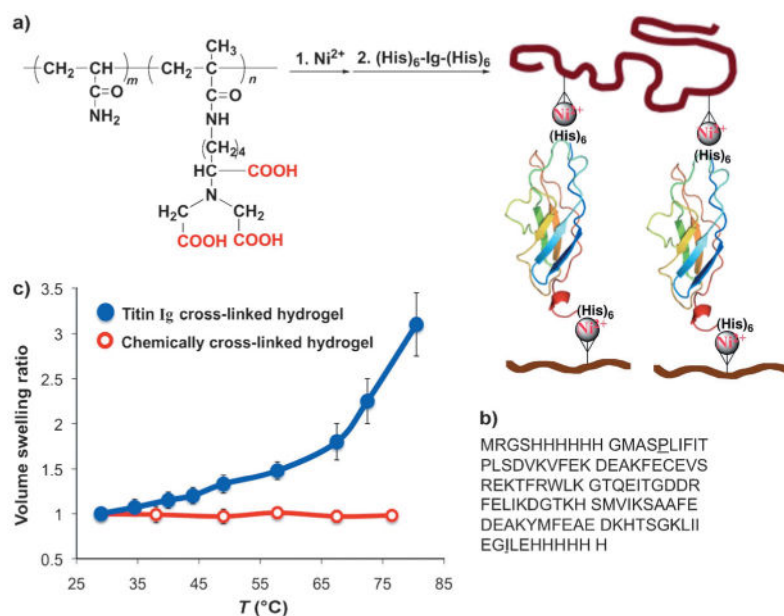


Figure 6. Poly(acrylamide)-based hybrid hydrogels self-assembled from acrylamide (AAM) copolymer and the (β -sheet) I28 immunoglobulin (Ig)-like module of human cardiac titin (an elastic muscle protein). The hydrogel was formed through metal complex formation by the pendant metal-chelating ligand, NTA- Ni^{2+} , on the polymer and the terminal His tags of the protein. a) Chemical structure of metal-chelating copolymer poly(AAm-co-2-methacrylamidobutyl nitrilotriacetic acid (MABNTA)). The polymer was prepared by copolymerization of AAM with the metal-chelating comonomer MABNTA in Tris buffer (pH 8.9) under nitrogen, using ammonium persulfate and N,N,N',N' -tetramethylethylenediamine as the redox initiator. b) Protein sequence of the recombinant titin I28 cross-linker $(\text{His})_6\text{-I28-(His)}_6$. The protein contains His tags at both ends. The underlined amino acid residues mark the start and end of the human cardiac titin I28 segment. The recombinant protein module contains 111 amino acids with a predicted molecular mass of 12.2 kDa. c) Temperature responses of hydrogels in phosphate-buffered saline (pH 7.2). The volume swelling ratio is the ratio of hydrogel volume at an elevated temperature to the volume at 29°C. Full circles: Titin $(\text{His})_6\text{-I28-(His)}_6$ cross-linked hydrogel; empty circles: methylene bis(acrylamide) cross-linked hydrogel. Adapted from Ref. [87].

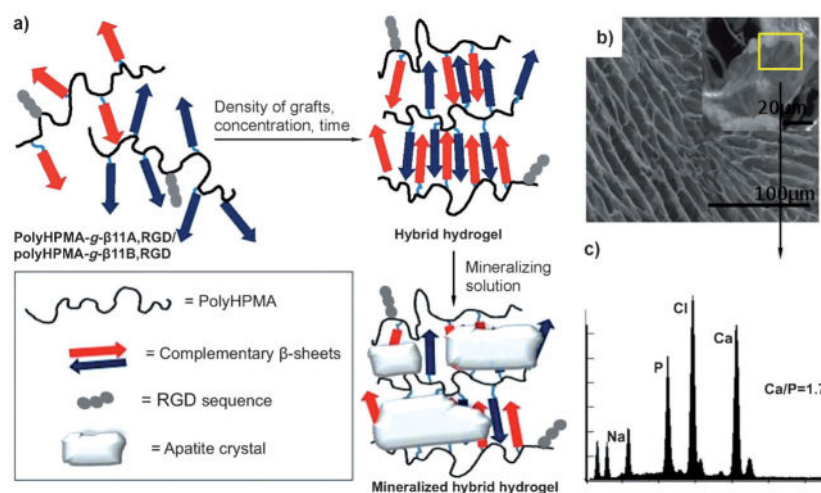
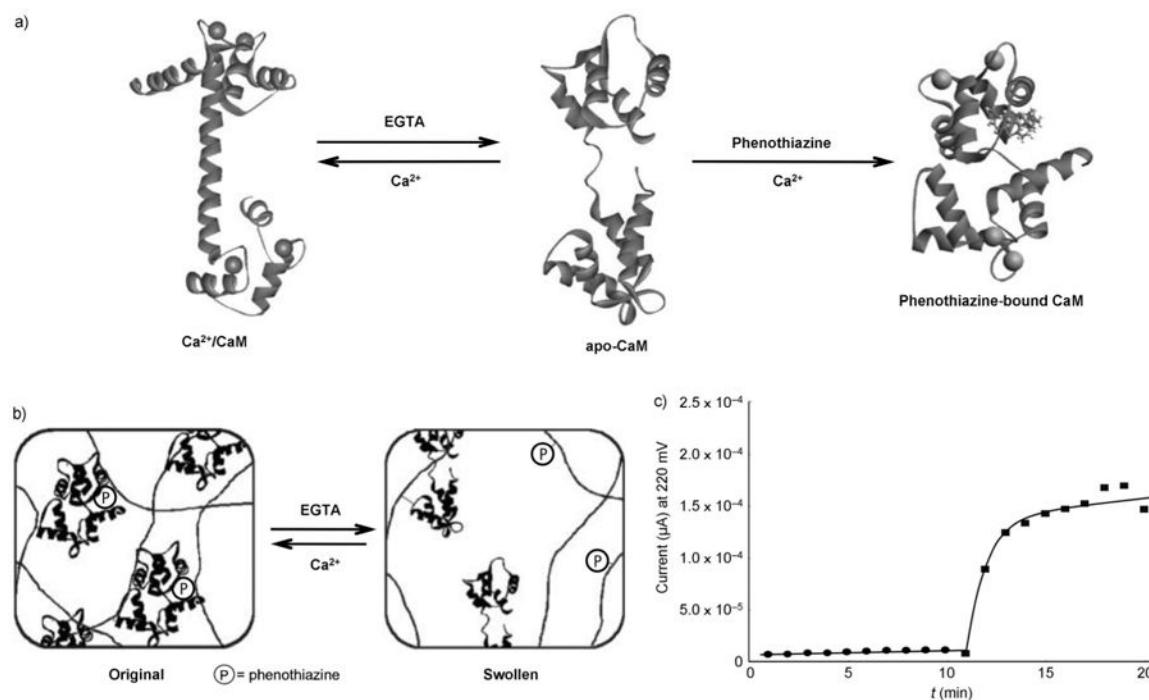


Figure 7. a) The self-assembly of HPMA graft copolymers containing complementary β -sheet forming grafts. b) SEM micrograph of (poly(HPMA)- g - β 11A,RGD: poly(HPMA)- g - β 11B,RGD) lyophilized hydrogel before mineralization; inset: SEM images of hydroxyapatite (HA) crystals deposited on the surface of poly(HPMA)- g - β 11A,RGD: poly(HPMA)- g - β 11B,RGD following exposure to simulated body fluid. c) EDS (energy dispersive spectroscopy) spectra corresponding to minerals (shown in inset of (b)) on the edge of the pores. Adapted from Ref. [152].

**Figure 8.**

Stimuli-sensitive hybrid hydrogel composed of acrylamide, methylene bis(acrylamide), and polymerizable derivatives of phenothiazine and calmodulin (CaM). a) CaM can adopt three different conformations: 1) dumbbell (Ca²⁺ bound); 2) native conformation (absence of calcium); and 3) phenothiazine and calcium-bound. b) Hydrogel structure at different conditions: EGTA (ethylene glycol bis(β-aminoethyl ether)-*N,N,N',N'*-tetraacetic acid) removes calcium from its binding sites. c) The efficiency of the hydrogel as a valve in a microfluidic system. ● valve closed, no release; ■ valve open, Ca²⁺ present. Adapted from Ref. [161].

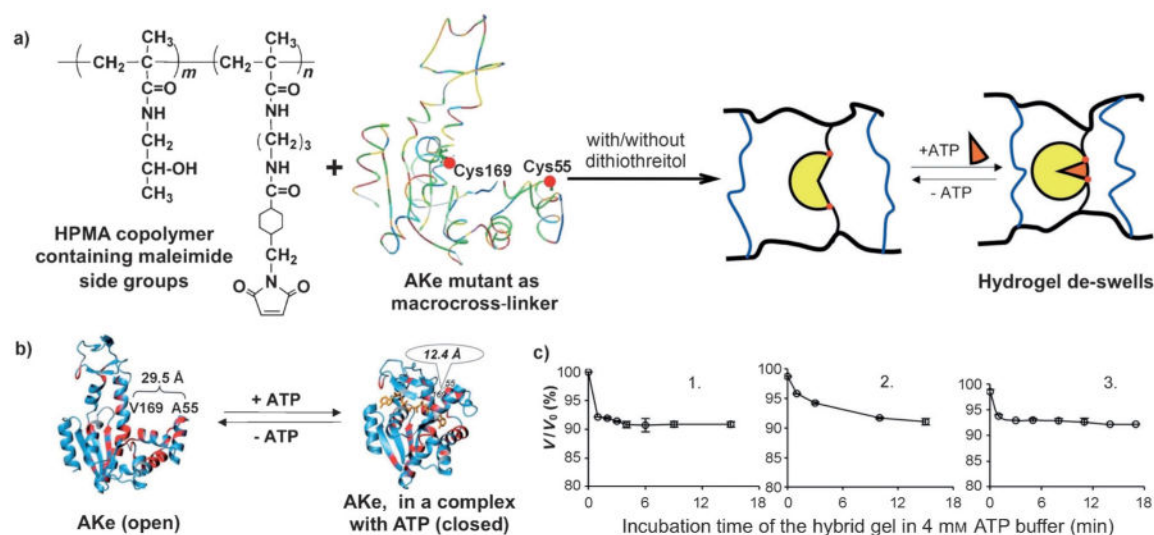


Figure 9. Hydrogels containing a triple mutant of adenylate kinase, AKtm (C77S, A55C, V169C), as a cross-linker are able to translate the enzyme conformational change upon binding a substrate into mechanical motion. a) Hydrogel forms by cross-linking of HPMA copolymer containing side chains terminated in maleimide groups with AKtm via thioether bonds formed by the reaction of Cys169 and Cys55 with maleimides. b) Ribbon diagram of the structure of adenylate kinase (AKe) in two conformational states: open state and closed state. c) Three cycles of deswelling of hydrogel cross-linked with 100% of AKtm. Adapted from Ref. [165].

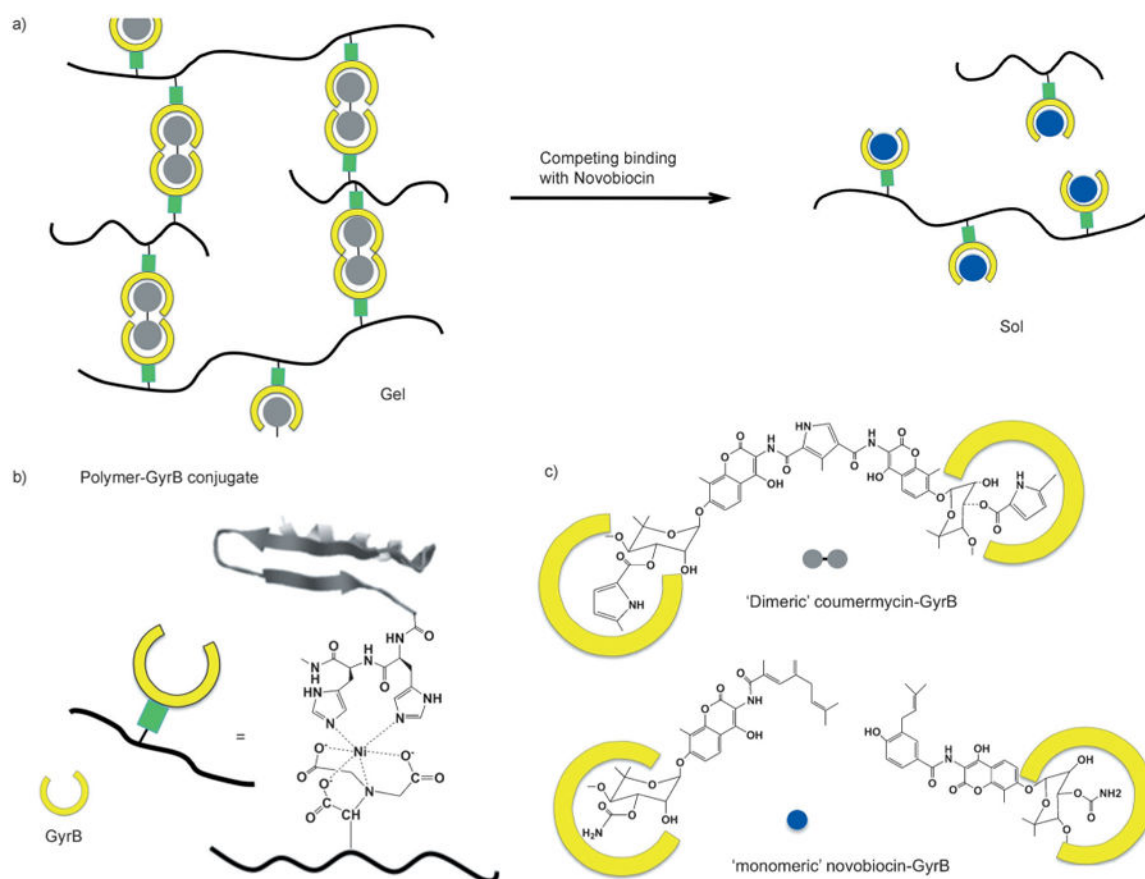
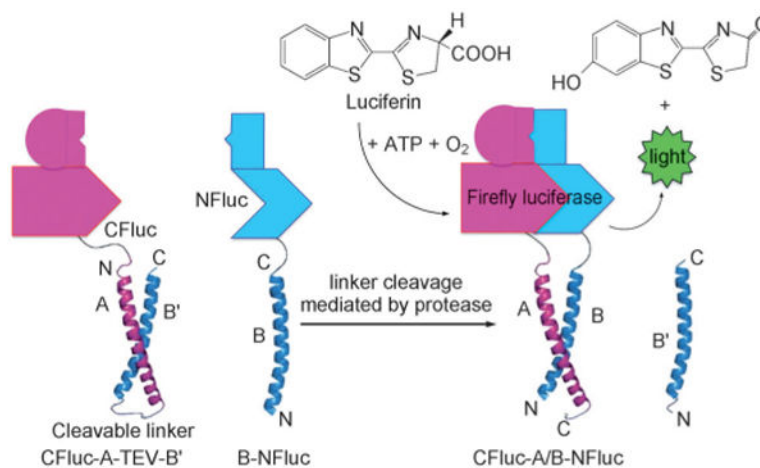


Figure 10.

Design and synthesis of pharmacologically controlled hydrogels: an antibiotic-sensing hydrogel for the trigger-inducible release of human vascular endothelial growth factor (VEGF). Genetically engineered bacterial gyrase subunit B (GyrB) coupled to polyacrylamide was dimerized by the addition of the aminocoumarin antibiotic coumermycin, resulting in hydrogel formation. Addition of increasing concentrations of novobiocin dissociated the GyrB subunits, resulting in dissolution of the hydrogel and VEGF release. a) Gel–sol transition by exposure of coumermycin crosslinked hydrogel to novobiocin; b) structure of polymer–GyrB conjugates; c) binding of GyrB with coumermycin and novobiocin. Adapted from Ref. [206].

**Figure 11.**

Turn-on protease biosensors based on an autoinhibited coiled-coil switch. Intramolecular coiled-coil cleavage results in split-protein complementation: the two firefly luciferase halves can reassemble into active protein that catalyzes the mono-oxygenation of luciferin to produce light. CFluc: C-terminal fragment of firefly luciferase (Fluc), residues 398–550; NFluc: N-terminal fragment of Fluc, residues 2–416. Helices A and B' comprise an intramolecular dimeric coiled-coil connected by a tobacco etch virus (TEV)-protease cleavage site. Adapted from Ref. [221].

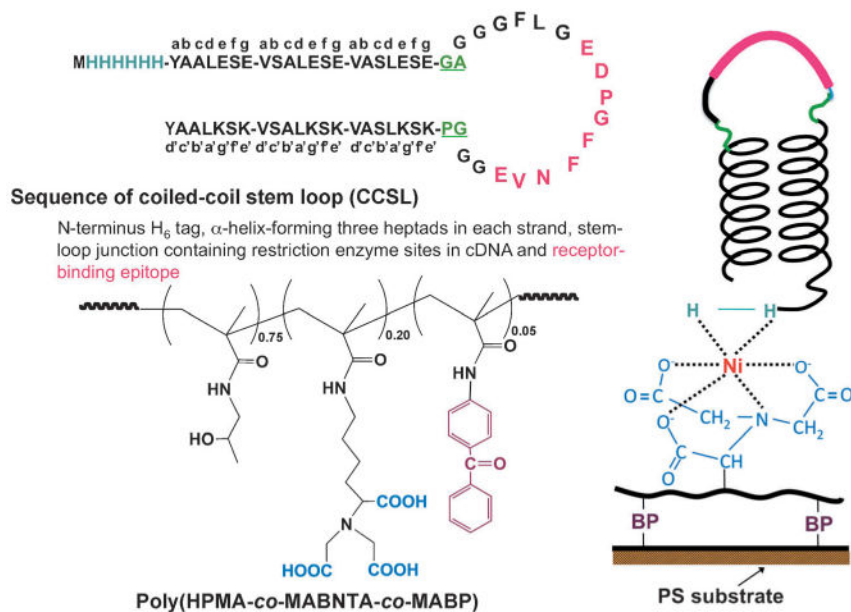


Figure 12.

Surface modification with self-assembled genetically engineered peptides exposing epitopes recognizable by human lymphoma cells. An antiparallel coiled-coil stem loop (CCSL) peptide self-assembled on a polystyrene cell culture dish, the surface of which was modified with HPMA copolymer containing nitrilotriacetic acid groups (NTA; to complex Ni²⁺) and benzophenone (BP) groups for covalent attachment to the surface. The biorecognition of the exposed peptide can be evaluated using CD21-positive B cells or the soluble CD21 receptor. Adapted from Refs. [234, 235].

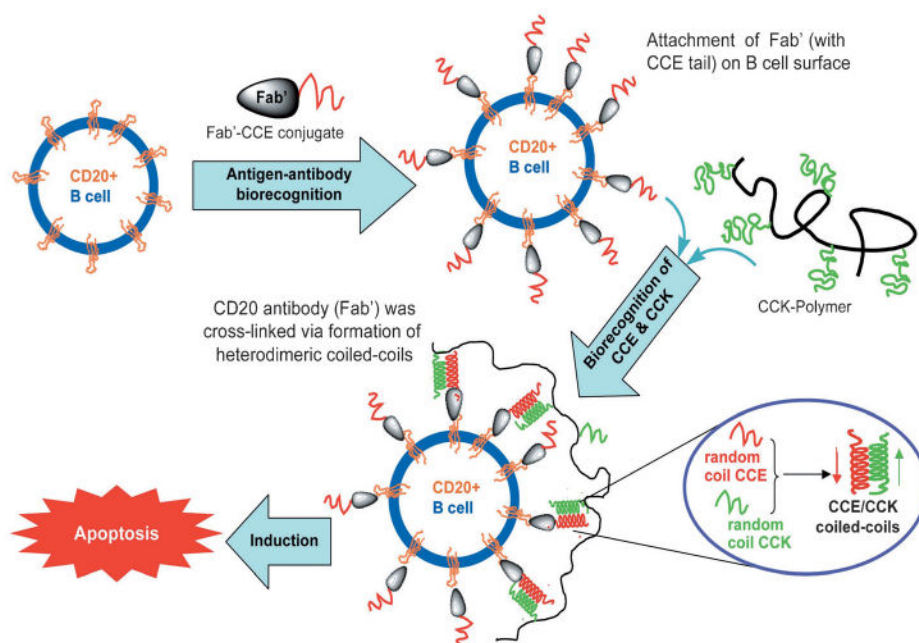


Figure 13.

Design of drug-free macromolecular therapeutics. Cartoon of overall design and possible mechanism of treatment of Non-Hodgkin's lymphoma (NHL) with conjugates of antiparallel coiled-coil-forming peptides, CCE and CCK. The induction of apoptosis in human Burkitt's NHL Raji B cells was triggered by cross-linking of the surface CD20 antigen owing to biorecognition processes of antigen–antibody fragment and complementary peptides. Exposure of Raji B cells to an anti-CD20 Fab'-CCE conjugate decorated the cell surface with CCE (CD20 is a non-internalizing receptor) through antigen–antibody fragment recognition. Further exposure of the decorated cells to CCK-P (grafted with multiple copies of CCK) resulted in the formation of CCE/CCK coiled-coil heterodimers at the cell surface. This second biorecognition induced the cross-linking of CD20 receptors and triggered the apoptosis of Raji B cells. Fab'-CCE is a conjugate of the Fab' fragment of the 1F5 antibody and the CCE peptide (YGGEVSALEKEVSALEKKNSALEKEVSALEKEVSALEK); CCK-P is a HEMA copolymer containing nine grafts of the CCK peptide (CYGGKVSALKEKVSALKEEVSANKEKVSALKEKVSALKE). Adapted from Ref. [250].

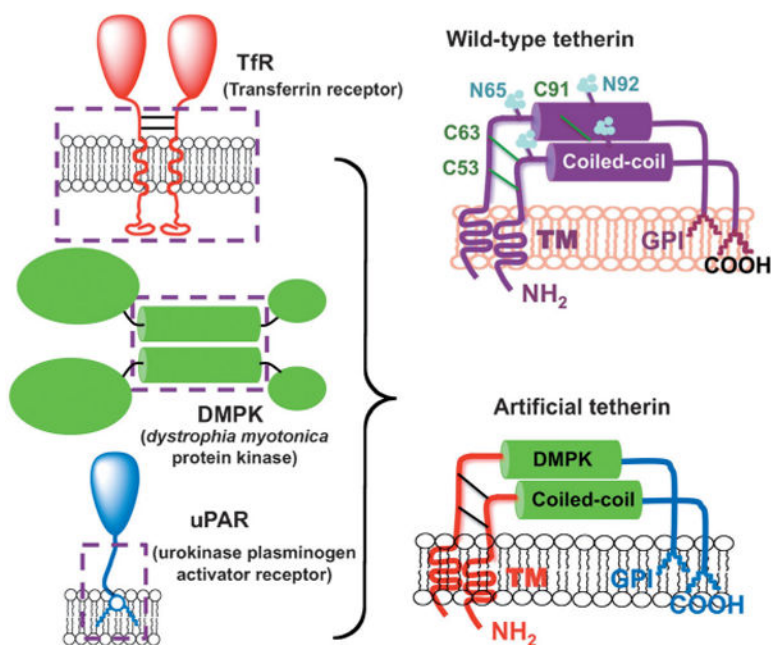


Figure 14.

De novo design of functional peptides/proteins. Replacement of functional domains of tetherin with analogous motifs from unrelated protein resulted in a functional construct. Artificial tetherin consisted of domains from the transferring receptor (TfR), dystrophia myotonica protein kinase (DMPK), and urokinase plasminogen activator receptor (uPAR). The fully artificial protein, lacking sequence homology with native tetherin, mimicked the antiviral activity of tetherin. Adapted from Refs. [255, 256].